3-10-2010

Minimizing Losses in a Space Laser Power Beaming System

Charlie T. Bellows

MINIMIZING LOSSES IN A SPACE LASER POWER BEAMING SYSTEM

THESIS

Charlie T. Bellows, Captain, USAF

AFIT/GSS/ENY/10-M02

DEPARTMENT OF THE AIR FORCE
AIR UNIVERSITY

AIR FORCE INSTITUTE OF TECHNOLOGY

Wright-Patterson Air Force Base, Ohio

AFIT/GSS/ENY/10-M02

MINIMIZING LOSSES IN A SPACE LASER POWER BEAMING SYSTEM

THESIS

Presented to the Faculty

Department of Aeronautics and Astronautics

Graduate School of Engineering and Management

Air Force Institute of Technology

Air University

Air Education and Training Command

In Partial Fulfillment of the Requirements for the

Degree of Master of Science (Space Systems)

Charlie T. Bellows, BS

Captain, USAF

March 2010

AFIT/GSS/ENY/10-M02

MINIMIZING LOSSES IN A SPACE LASER POWER BEAMING SYSTEM

Charlie T. Bellows, BS

Captain, USAF

Approved:

_____ signed _____	_____
Jonathan T. Black, PhD (Chairmen)	Date
_____ signed _____	_____
Richard G. Cobb, PhD (Member)	Date
_____ signed _____	_____
Salvatore J. Cusumano, PhD (Member)	Date

Abstract

A mathematical model is developed to track the amount of power delivered in a wireless laser power beaming system. In a wireless system the power proceeds through several different stages before being delivered to a payload for use. Each of these stages results in power losses that are thoroughly examined and modeled, allowing for the calculation of the likely amount of power delivered. Adjusting variable factors within the model allows for the optimization of the system for a specific task. The model shows that an optimized wireless power transfer system can deliver enough power to meet the space experiment objectives. For example, to power a Hall-Effect Thruster, a laser, photovoltaic cells, satellite power distribution method, and batteries all impact the amount of power delivered. Careful selection of these components will allow the laser to power the thruster and the model provides how much power is transferred. Knowledge of the power requirements for the payload allows the model to determine how long it will be able to operate the payload with the power provided. This model will allow system engineers to answer important design questions about the selection of components to ensure that the end product delivers maximum power.

For my Wife

Acknowledgments

I would like to acknowledge and thank the following people for their help and support in completing this research: my faculty advisor Dr. Jonathan Black for his continued guidance throughout the effort, and Dr. Salvatore Cusumano for increasing my knowledge of lasers and their control systems. I would also like to express my appreciation for J Simmons for teaching me to use Model Center as a tool to test the model and Mr. Rick Bartell for independent verification of the working model. Finally my gratitude is due to Elizabeth Y for the illustrations created for this work.

Charlie T. Bellows

Table of Contents

Page

List of Figures

Page

List of Tables

Page

MINIMIZING LOSSES IN A SPACE LASER POWER BEAMING SYSTEM

I. Background

1.1 Motivation

The concept of wireless power transfer through electromagnetic waves has been around for some time. It has even been argued that the ancient mathematician Archimedes conceived this technology during the Punic wars of 214-212 B.C. when he focused sunlight onto enemy ships to set them ablaze (Perram, 2009).

In more recent history the inventor Nikola Tesla proposed a wireless power transfer system for the purpose of powering electric objects like light bulbs, as early as 1893 (Cheney, 1989: 61). He argued that electric potential differences could be created in the air in such a manner as to create an electric current that could then be used to light a neon gas tube, or fluorescent light bulb, anywhere inside the current without it being connected to any other power source. He believed that this was a more efficient manner in which to power modern conveniences than running wires through walls or along ceilings and floors. This Tesla Effect can be easily demonstrated using a Tesla Coil to ionize air particles and create a current in a modern fluorescent tube. Once the device has been turned on simply holding the tube on one end and pointing it at the device will light the tube to the location of one's hand, in this case the person holding the light also acts to ground the system. This method of powering devices never caught on, but recently another device for wireless power transfer has been proposed.

In 1958 Arthur Schawlow and Charles Townes were credited with the invention of the first laser by Columbia University which they patented in 1960; however, the first working laser was created by a Theodore Maiman later that year (Perram, 2009).

With the invention of the laser and the development of both photovoltaic and thermal power system technologies the concept of wireless power transfer has been revisited in recent years. In 1994 NASA, along with the International Society for Optical Engineers (SPIE), began investigating applications for wirelessly powering space assets from the ground using electromagnetic waves (SPIE, 1994). With a recent push for renewable green forms of energy, organizations have been looking at reversing this concept in order to beam power to the ground from deployed space assets (Mankins, 2008:20). In fact a recent Wall Street Journal article listed space-based solar power as one of "Five Technologies that Could Change Everything (Totty, 2009)." Furthermore this technology has applications for Man's return trip to the moon, as powering lunar missions through the 354 hour lunar night could be done using the same wireless power systems developed for use on or around the Earth (Landis, 1994:253).

The purpose of the NASA wireless power transfer experiment purposed is to prove the validity of wireless power beaming in space by transferring power from one orbital vehicle the International Space Station (ISS), to another orbital vehicle, a satellite. This experiment faces many of the challenges shared by all wireless power beaming experiments, including the need for highly efficient power transfer technology in order to minimize losses, systems that can stand up to the high temperatures incurred under the fluence of an optical transfer system, and safely transferring the power from one platform to another without interfering with a third party.

In the proposed experiment a small satellite will be launched into low earth orbit (LEO) and a high energy laser will be placed on board the International Space Station. Specifically the laser would be attached to the Japanese Experimental Module (JEM) External Facility (EF) where it would be provided with 3 kW wall plug power. The satellite, tentatively based on the FalconSAT 5 design, will function as the recipient of power beamed from the space station. The power transfer itself will be performed using the laser to send power and photovoltaic's to collect the power at the satellite. Power losses from the transfer are expected and should be in keeping with current technological limitations.

Efficiency is a key component of any power system. Minimizing losses becomes even more important when dealing with a photovoltaics industry where 25% efficient components are incredibly good (IPG Photonics Corporation, 2009a:2) (Space Technology Library, 2008:414). When looking at wireless power transfer many systems are stacked upon each other to the point that the system of systems is expected to have less than 10% efficiency. When expecting 90% losses, great attention to detail should be paid in the selection of components to eliminate every possible loss of power to maximize the overall system efficiency.

1.2 Problem Statement

No accurate model of the power transfer exists. Current loss calculations have been limited to napkin equations in order to determine a best guess. This leads to disconnects between engineers working on designing the laser and those working on the

design of the satellite. This thesis is an initial attempt to ensure that the system is optimized in order to transfer the maximum amount of power in space.

A well-developed power transfer model would be able to answer system level design questions ensuring that all power losses are accounted for and minimized in order to achieve maximum power delivery to the satellite.

1.3 Research Objectives

The research objective of this thesis is to model the power transfer system for an in space laser power beaming experiment. The model will mathematically show power losses from the 3 kW power source on the International Space Station through to the use of that power by a Hall Effect Thruster on the target satellite. This model can then be used to help design a feasible power transfer experiment.

The model will be used to determine the best components or combination of components for the Laser Power Transfer System to minimize the power losses and maximize the overall efficiency. To optimize the system, the peak frequencies of the photovoltaic subsystem and the power laser subsystem will need to be determined. The losses caused by each subsystem will also need to be examined to determine if there is a more efficient component that can be used instead. These subsystems include the laser, the components of the laser system such as the fast steering mirror, and components of the satellites electronic power subsystem such as solar cells, wiring, and electric convertors.

1.4 Investigative Questions

The main questions this research seeks to answer are:

- What combination of laser and photovoltaic cells provide the best efficiency and performance for the NASA wireless power beaming experiment?
- What Power Management scheme should the satellite use for the experiment?
- What are the power losses caused by each subsystem, and does a more efficient potential replacement exist?
- What effects do range, contact time, atmosphere, and sunlight have on the power transfer?

The answers to these questions all have an impact on the amount of power wasted in the system. Answering them accurately will lead to a better understanding of the design requirements which in turn will lend itself to a better system overall.

A secondary objective of this research is to determine if there are their long-term wireless power transfer applications in future space, ground, or lunar missions? Knowing the answer to this question paves the way for future endeavors to utilize this technology.

1.5 Overview

To answer the questions above, a literature review will be conducted in Chapter II. Literature Review covering applications of wireless power transfer systems, the basic aspects of laser technology, and photovoltaic science. This knowledge will be used in

Chapter III. Method to build and test a model that accurately portrays the amount of power transferred. In Chapter IV. Analysis the findings of the test plan will be presented to demonstrate that the model works correctly. Finally in Chapter V. Conclusions and Recommendations the answers to the research questions will be presented and any future research required will be listed.

II. Literature Review

The purpose of this chapter is to provide an overview of the topics involved in wirelessly beaming power in space, as well as a summary of related research. The review begins with an overview of applications that the community has already explored in Sect. 2.1. It continues by covering lasers devices that may be considered along with a discussion of current laser technology suitable for this experiment in Section 2.2.1. Finally how the satellite might collect the power from the laser system is considered in Section 2.4.

2.1 Laser Power Transfer Applications

As mentioned in Sect. 1.1, SPIE held a series of speaker conferences in the mid 90's to consider possible applications for wireless power transfer systems in space experiments. Some of the topics of interest that they developed include powering satellite vehicles, powering electric propulsion, debris removal and renewable energy for the ground. Each of these topics is discussed in detail below.

2.1.1 Renewable Energy for the Ground

The most popular vision of space-based power is a constellation of on-orbit collectors used to gather solar energy directly from the sun and then "beam" that energy down to large receivers on the ground in order to provide power.

Earth-generated solar energy is not currently enough to sustain future clean energy power needs, or aid in satellite power requirements, as energy output of a conventional ground-based solar array is reduced by as much as 80% by the atmosphere, masking angles due to local terrain, nighttime and weather (Mankins, 2008:20). Space-based solar power can address all of these needs simultaneously, but there are several challenges that need to be tackled before it will be a reality. Thankfully these obstacles can be overcome by engineering and economics, and the basic technology has been around since the late 1960's (Mankins, 2008:25).

The challenges that need to be overcome include the need for highly-efficient electronic devices that can operate at high temperatures, delivering precise and safe wireless power transmission, dramatically lowering the cost of the space systems and operations, and achieving low-cost access to space (Mankins, 2008:22-25). Working to overcome these challenges, the Japan Aerospace Exploration Agency (JAXA) intends to launch a Space Solar Power experiment by 2030 (Gingichashvili, 2007). The experiment will use a Neodymium solid state laser similar to the devices discussed in Sect. 2.2.2.

The concept of gathering solar energy and beaming it to a receiver can also be applied to power space faring vehicles near Earth which are constrained by power and fuel requirements.

2.1.2 Powering Satellite Vehicles

Satellites on orbit periodically go through the shadow of the Earth creating a solar eclipse. The frequency and length of such eclipses depended on altitude of the orbit, its

inclination and the time of year. During such eclipses the satellite no longer receives power from its photovoltaic cells and must instead rely upon internal batteries for power.

Low Earth orbiting satellites experience the most frequent eclipses, potentially experiencing more than 18,000 eclipses each year. Geosynchronous satellites, such as communications satellites, are only in eclipse for about 90 days a year around the vernal and autumnal equinoxes. The max eclipse duration of such a satellite is around 70 minutes.

In a geosynchronous satellite, the electrical power subsystem is about 1/5 of the total mass and half of that serves only to store energy for the less than 1% of the mission time when the vehicle is in eclipse (Landis, 1994:253). Eliminating the need to store power onboard by using an external laser source to power the vehicle during eclipse could reduce the mass of the vehicle by 10% (Landis, 1994:253). Even current on-orbit satellites using Nickel Cadmium batteries can benefit from laser power being provided during eclipse.

Rechargeable Nickel Cadmium batteries have a lifespan determined by the number of times they can successfully be charged. The more often a battery must be charged, the shorter its life will be. The amount a battery must be charged is determined by the amount of discharge it experienced during the eclipse. If a laser could be used to limit or remove this discharge altogether then the life of the battery would be lengthened as would the life of the satellite that depends upon it.

Using laser power to reduce or eliminate battery discharge for a satellite in any orbit from beginning of life could drastically increase its lifetime. Even beginning to use laser power beaming technology partway through a satellites life can be used to increase

the life span (Monroe, 1994:258). It should be noted that only Nickel Cadmium (NiCd) batteries can benefit from DoD reduction applications as Nickel Hydrogen (NiH_2) batteries last so long that they are not the limiting life cycle factor on board (Monroe, 1994:261); however, that does not mean that future satellites intended to use NiH_2 cannot benefit from this technology. As mentioned above appropriately placed power stations on orbit could eliminate the needs for batteries altogether, lowering satellite mass and reducing launch costs.

Reducing the need to carry batteries is not the only way a wireless power system could potentially help a satellite; it could also be used to power electric propulsion units which can require more power than the photovoltaics alone can provide.

2.1.3 Powering Electric Propulsion

Ion engines and other electric propulsion systems have considerably high specific impulses[1] which could dramatically effect in-space transportation from small station keeping maneuvers to longer orbital transfers. In addition they are incredibly efficient and require much less fuel than more traditional chemical engines; however, they also have high power requirements. Using a laser-based power transfer system to increase the power available to such a propulsion system can drastically enhance the performance of such a system possibly even decreasing the transit time of a satellite transferring from low earth orbit to GEO by a factor of three (Landis, 1994:253).

[1] Specific Impulse of 300 to 5,000 sec (Space Technology Library 2008:703)

In the article *Scaling of Solid State Lasers for Satellite Power Beaming Applications* the authors suggest that a common Neodymium: yttrium aluminum garnet laser, a type of solid state laser, is suited for laser-powered delta V, a change in velocity used to either maintain the space vehicles current orbit, or move it into a different orbit, early in a vehicle's lifetime, before on-orbit degradation of the solar cells lowers the efficiency below a usable level (Herbert Friedman, 1994:50). Powering space systems remotely has potential benefits both for electronic power subsystem (EPS) systems and propulsion systems, but this is not the only way lasers can be beneficial to space missions. Creative applications of lasers may also be used to solve other long term problems such as the concern over growing space debris.

2.1.4 Debris Removal

Space debris is a considerable problem for modern day space operations and there are those who believe that the problem will drastically increase (Wiesel, 2009) in coming years. For this reason the prospect of using lasers to remove space debris is an appealing side application of any high powered laser. It is particularly of interest in the orbit of the ISS whose size, and the level of activity in its region of space, makes it a likely candidate for collisions with space debris.

The method used for clearing space debris with a laser is to push a piece of debris in a direction normal to its orbital velocity. This push creates a change in the location of apogee and perigee which if done correctly can cause the debris to intersect the Earth's

atmosphere (Monroe D. K., 1994:278-279). Furthermore, several passes of the unwanted debris through the laser's field of view may be required to effectively destroy the object.

The laser power beamed from the ground required to move a piece of debris enough to cause it to reenter the Earth's atmosphere is considerably high, multi-megawatt for a 1 kg object (Monroe D. K., 1994:277-278). Some of that power requirement however is due to atmospheric losses that an orbiting laser would not experience. Unfortunately there are many dangerous and un-cataloged pieces of debris that would remain immune to debris removal activity, even if a laser is capable of performing such a task, as they are too small to track (Wiesel, 2009). Never the less, removal by any means of any quantity is a step in the right direction (Cobb, 2010).

2.1.5 Summary

A high power utility laser on orbit can be used to power ground applications, power satellites through eclipse, provide power for electronic propulsion systems on board space vehicles, or even remove dangerous space debris. Different types of lasers are best suited for each mission but a well rounded high power laser can work effectively for most missions as discussed in Sect. 2.2.2.4.

2.2 Methods for Wireless Power Transfer

Methods for transferring power into the far field, a distance greater than the size of the device transmitting power or a quarter of the wavelength used to transfer the power, can be done in a handful of ways.

As early as 1926 a device designed to use radio-waves to transfer power had been built and tested; however the longer wavelengths made it difficult to direct the power and the system was to inefficient for any practical power transfer applications (Reiman, 1993:2). Shorter wavelengths are easier to direct and have led to the development of the rectenna, a device design to convert microwave energy into electricity.

Microwave power transmission has been experimented with since the mid 1970's successfully demonstrating power transfers in the tens of kilowatts over distances greater than a kilometer. Unfortunately the equipment involved in microwave power transfers tends to be quite large. As with radio waves, the pointing requirements require kilometer sized arrays for both transmitting and receiving in order to overcome diffraction losses See section 2.2.2 below, associated with the long wavelengths of microwaves (Microwave Antenna Theory and Design, 1984: 40-43). This large equipment requirement limits the usefulness of microwave energy as the medium for power transfers between satellites.

Lasers on the other hand seem suited for laser power beaming in a vacuum as they can be small enough to launch on space vehicles and the collection method (photovoltaic) is already in place for current satellites and they will not interfere with radio-based satellite communications.

2.2.1 Lasers

As a laser is the best means of transferring power for a space power beaming experiment, research into the available laser technologies is presented below. Three different types of laser devices, free electron lasers, solid state lasers, and fiber lasers are explored in order to determine the best fit for an on-orbit laser. Each type of device has its advantages and disadvantages, which are explored below.

2.2.2 Laser Basics

The word laser comes from the phrase light amplification by the stimulated emission of radiation. A laser beam is created by a device that stimulates electrons of an atom into a state of increased energy so that when the electron returns to its original state it emits a photon. The photons that are emitted from a laser device are all of a single color and move in a single direction in a coherent manner.

The quality of the beam produced will determine how useful the laser is in a wireless power beaming application. Diffraction of the laser beam will naturally occur as lasers deal with very small scale phenomena (such as photons) and cannot be avoided, but other causes of beam degradation also exist. Beam quality is represented in the laser community by the M^2 number. An M^2 value equal to one is referred to as being diffraction limited[2] and values greater than one indicate a laser beam that performs worse

[2] Diffraction limited implies that diffraction effects are the only cause of degradation of the laser beam.

than diffracted light. Laser device manufactures strive to create laser devices near diffraction limited performance.

Laser devices consist of optical resonators, which include a gain medium excited by an external energy source, and two mirrors as shown in Figure 1.

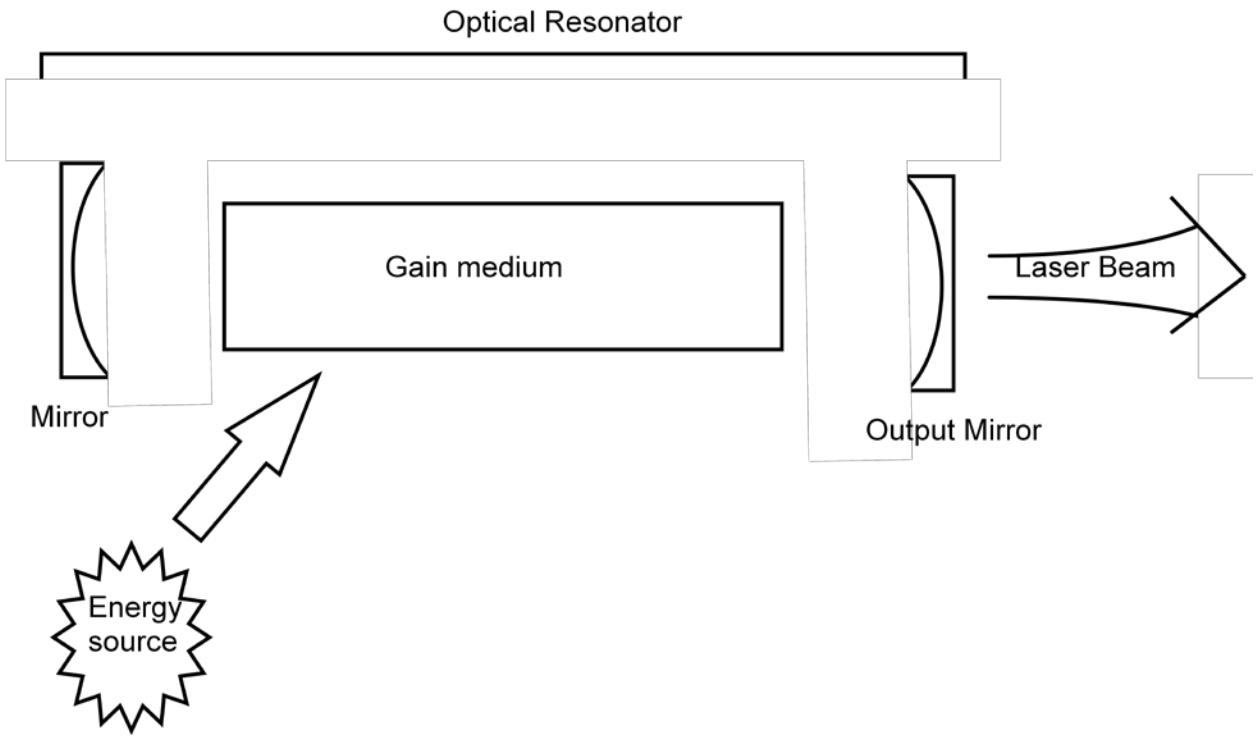

Figure 1: Laser Device (Perram, 2009)

The first of the two mirrors is completely reflective, while the second of the mirrors is only partially reflective. This ensures that the photons exit in a single direction and serves to further excite electrons in the gain medium using the moving photons already present. As more electrons are excited and then return to their original state, only to be excited again, more photons are released into the laser beam.

As electrons are excited and release photons, not all photons will be at the same wavelength. As the light of different wavelengths interacts with one another inside the cavity of the laser both constructive and destructive interference will occur, as a result of this interaction only photons with round trip distances inside the cavity equal to an integer multiplier of their wavelength can continue to propagate inside the cavity. Each possible wavelength will be separated from other possible wavelengths with nearly even spacing and are the possible modes of the laser (Meschede, 2007:101).

The number of electrons that can be excited at any given time is limited by the threshold of the gain medium. Saturation occurs when gain caused by stimulated emission equals the losses in the system (Meschede, 2007:301-302). This is referred to as saturated gain, gain clamping, and saturation flux in the reviewed literature. There are additional important laser properties that will be discussed as required with each type of laser reviewed below.

2.2.2.1 Free Electron Lasers.

A free electron laser (FEL) is defined as a device for generating coherent light by sending a relativistic electron beam through an oscillating magnetic field. A FEL has three fundamental components: an electron beam of given energy and intensity and the associated accelerator used to produce it, the magnet which cause the particles of the electron beam to oscillate creating an interference pattern, and finally the EM wave and optical components controlling its propagation (Perram, 2009).

In the literature, the free electron laser is a prime candidate for the laser power beaming experiment for several reasons. First the interaction of electrons inside the magnetic field increases energy spread which removes waste heat from the system at relativistic speeds, cooling the system as it is being used and eliminating the need for an independent cooling system. Furthermore, unlike chemical or solid state lasers the electron beam cannot be damaged by the "very high optical intensities which are needed in a high-power FEL (Goldstein, 1995:32)" allowing the system to use more power than a solid state laser which must keep its power levels low enough to ensure that it does not damage the internal workings of the laser. However, high efficiency (η) for such devices is considered to be 10% (Goldstein, 1995:34), which is considerably lower than the efficiencies of the solid state lasers.

2.2.2.2 Solid State Lasers

Solid state lasers tend to come in three varieties; the flash lamp pumped, diode lasers, and diode pumped solid state lasers. They work by exciting electrons in a crystal, or laser rod, such as Neodymium: Yttrium Aluminum Garnet (Nd:YAG), using either a lamp or diodes to pump energy into the medium. This excitation then results in lasing as electrons fall from there excited state back to a state of rest only to be excited again. This cycle creates a usable laser beam (Perram, 2009).

Two technical problems may prevent this type of laser from being considered for space power transfer applications. The first of these problems is that wavelength of efficient solid state lasers are above one micron which makes them highly inefficient for

transferring power to solar cells typically designed with a peak efficiency of 500 to 600 nm (see Sect. 2.4). The second problem is the historical inability to attain high average powers with good beam quality (Herbert Friedman, 1994:49) which significantly limits the range of solid state lasers.

Two possible solid state lasers for laser power beaming to a satellite are Alexandrite and Thulium: YAG (TM:YAG). The wavelength of the Alexandrite laser is centered at 680 nm, provided by the chemical properties of the Alexandrite; however, Alexandrite has a saturation flux of 150 kW/cm^2 which is 60 times greater than that of the more standard Nd: YAG (Herbert Friedman, 1994:51).

> This means that to reach sufficient gain to keep the gain/loss ratio large and hence result in high extraction efficiency, high pump power densities must be developed. High pump power densities will result in large waste heat loads and concepts such as pressurized coolant systems, which can take full advantage of the large thermal shock parameter, must be used. Even with these considerations, the gain and therefore extraction efficiency of Alexandrite lasers will be low unless long crystals can be manufactured (Herbert Friedman, 1994:51).

Thulium-doped YAG has been demonstrated at a wavelength of 1.92 micrometers (Herbert, 1994:50); however, it is possible to use an intense pumping method which causes the laser to output a beam with wavelength of 780 nm (Herbert Friedman, 1994:54). This method requires the development of reliable coatings for the gain medium that will handle average gain saturation at the required intensity.

Both laser options would require the use of laser diode arrays and optical compression in order to ensure the proper power output and a usable beam. The power

output in each case is in the neighborhood of 30 kW (Herbert Friedman, 1994:51-54), requiring an input power of roughly 50 kW for the Alexandrite and over 150 kW for the pump driving the Tm: YAG.

The efficiency of these lasers appears to be driven by current laser diode array efficiencies which have been measured as high as 60% (Herbert Friedman, 1994:50). Unfortunately laser diode arrays create a waste heat load of 1 kW/cm^2 (Herbert Friedman, 1994:50) and Alexandrite generates 150 W/cm^2 for a 5 mm thick slab, and pressurization is therefore required to insure proper cooling. Since pressurization is not necessarily an option in the vacuum of space a more realistic option such as a fiber laser should be explored.

2.2.2.3 Fiber Lasers

A fiber laser is a type of solid state laser in which laser light is sent down the core of a fiber optic cable; the outer cladding is then pumped with light, the light passes back and forth through the core exciting the laser energy as it progress. The result is a usable laser output that can be as powerful as a 100 kW as shown in Figure 2.

The realization of high power fiber lasers, with power outputs greater than 1 kW and M^2 values less than 1.5, see Sect. 2.2.2, have made it clear that fiber lasers represent one of the most promising solid state laser technologies yielding high output power with superb beam quality. Typical operating range for such a laser is 1060-1110 nm, which is higher than desired for a space power beaming experiment as current photovoltaic cells

are designed for sunlight and thus have better quantum efficiencies near 500-600 nm (see section 2.3 Photovoltaic Power Collection).

The article *242W Single Mode CW Fiber Laser Operating at 1030nm* discusses the design of an Yb-doped fiber laser designed to operate at 1030 nm wavelength (Victor Khitrov, 2005:1). This design is intended to explore shorter wavelength solutions for a number of emerging applications in the field of lasers. The results of the experiment show an overall efficiency of the laser around 73%, better than any type of laser discussed so far. The beam itself was very close to being diffraction limited at M^2=1.05, furthermore the laser had a narrow spectral line width of only 0.35 nm and no sign of detrimental non-linear effects were observed (Victor Khitrov, 2005:3).

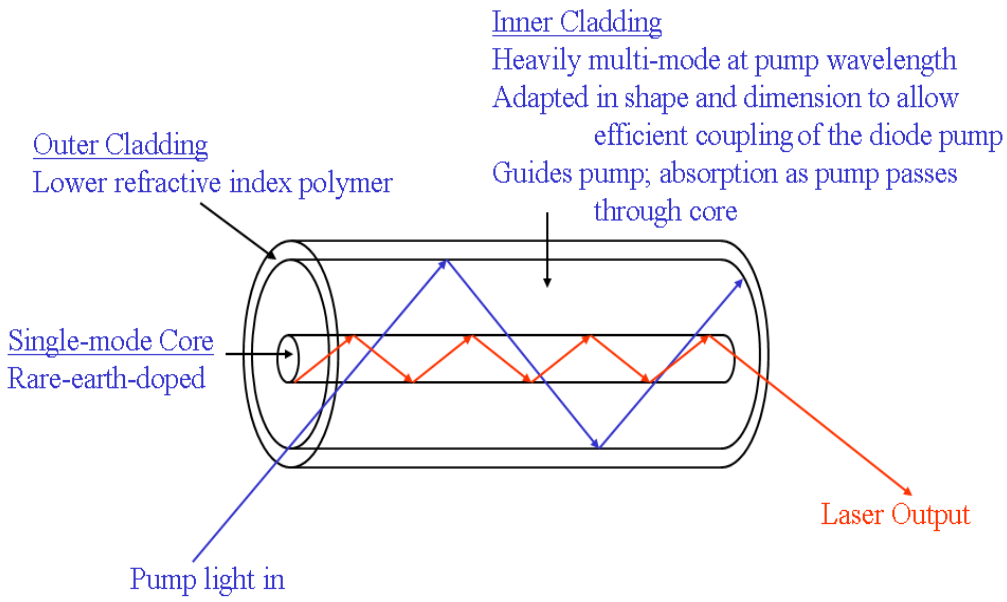

Figure 2: Fiber Laser Diagram (Perram, 2009)

It was also noted that these experiments stayed well below the glass-damaging power level in the fiber, and modeling indicates that it could handle up to 2 kW of power before damaging the laser itself. It is possible that a similar laser could be designed to handle up to 10 kW of wall plug power, which means that in the near future these highly-efficient lasers may be scaled up to the 3 kW level of power available on the ISS (Victor Khitrov, 2005:3).

2.2.2.4 Available Laser Technology

The available laser technology for this experiment has now been discussed in detail; however, for a laser to be usable by this experiment it must be able to accept 3 kW of wall plug power, fit in the volume allotted by the External Facility (EF) on the Japanese Experimental Module (JEM), 1.85 m x 0.8 m x 1 m (Fork, 2008), have near diffraction limited beam quality, and as high an efficiency as possible.

With these considerations in mind, fiber lasers quickly become the best option. The use of active optical fibers "allow for an extremely bright light out of a very small core (IPG Photonics Corporation, 2009a:4)" that not only provides excellent beam quality, it keeps the laser small enough to fit within the confines of an EF experimental module payload. A high-power fiber laser is further improved by the use of bright semiconductor-single-emitter-diodes which pump the fibers giving a longer system "lifetime compared to lamp or diode bar/stack pumped systems (IPG Photonics Corporation, 2009a:4)." One final benefit is afforded when you combine these two technologies:

> The combination of both technologies results in a unique, highly reliable and extraordinary performance laser system with parameters exceeding any traditional laser technology, including disc or rod YAG and CO_2 lasers (IPG Photonics Corporation, 2009a:4).

In addition to meeting weight and volume requirements imposed by the JEM "The high beam quality and efficiency of fiber lasers make them ideal candidates for directed-energy applications (Sprangle, Ting, Joseph, Fischer, & Bahman, 2008)." High power fiber lasers have an efficiency greater than 25% and near diffraction limited beam quality (IPG Photonics Corporation, 2009a:2) (Sprangle, Ting, Joseph, Fischer, & Bahman, 2008), making them well suited for this experiment.

Several high-power lasers can be commercially purchased, but multiple sources all indicate that IPG Photonics in Oxford, MA is the industry leader in fiber lasers (Sprangle, Ting, Joseph, Fischer, & Bahman, 2008) (Cusumano, 2009) (Fork, 2008) (Bartell, 2009). A proposed design for this experiment states that both an IPG Photonics and SPI Lasers (Southhampton UK) laser would work, and Sprangle, et al. names another company, Nufern in East Granby, CT, as a builder of fiber lasers that may meet the experimental requirements.

> These multikilowatt single-mode fiber lasers are robust, compact, nearly diffraction-limited, have high wall-plug efficiency, random polarization, and large bandwidth. A 1 kW single-mode IPG fiber-laser module, emitting at 1.07 μm, has a dimension of approximately 60 × 33 × 5 cm (excluding power supply), weighs about 20 lb, has a wall-plug efficiency of about 30%, and has an operating lifetime in excess of 10,000 hours (Sprangle, Ting, Joseph, Fischer, & Bahman, 2008).

Another possibility is to use a Japanese-made laser similar to the one JAXA is using in their Space Solar Power experiment. As covered in Sect. 2.2.2.2, Neodymium solid state lasers have high efficiency rating and good beam quality at higher powers, 50-150 kW wall plug power or greater. For the multi-gigawatt laser Japan envisions (Gingichashvili, 2007) this power level is appropriate, but it is unlikely that it would achieve near diffraction limited performance with only 3 kW wall plug power.

Nufern does not actually make any Kilowatt-class lasers. The company specializes in optical fibers (Nufern, 2004) and makes a series of lower power level fiber lasers and a kilowatt amplifier. The Nufern Kilowatt Level Laser Amplifier Platform is designed for beam combining applications and produces a near diffraction limited beam (M^2=1.2) but has an effective power delivery range of only 10 meters (Nufern, 2009:2).

The SPI lasers also have good beam quality (M^2= 1.3), a wavelength of 1.07 μm, and are 30% efficient, but has a rated power output of 400 Watts (SPI Lasers, 2009:1). This will limit the input power to only 1.3 kW, less than half of what is available, or risk damaging the laser.

IPG Photonics sells a series of lasers at the kW level. Specifically their YLR 1000SM appears to meet the needs of this experiment. The laser is a single mode fiber laser with 25% wall plug efficiency, near diffraction limited beam (M^2=1.1) performance, a wavelength between 1.06 and 1.08 μm, and it is capable of handling a 3kW input power (IPG Photonics Corporation, 2009a:3). This laser is 60cm tall by 80cm wide and 80 cm long, small enough to fit inside a JEM, EF payload and still leave room for focusing and corrective optics, and it weighs only 150 kg. This laser not only appears to be the best-suited for the power beaming experiment; it also appears to be the only laser that meets

all of the mission needs. Knowing what laser will most likely be used allows for the educated pursuit of the power collection source for the satellite.

2.3 Photovoltaic Power Collection

2.3.1 Photovoltaic Cells

Photovoltaic cells, also referred to as solar cells if the source of light is the sun, work by converting light into electricity using the photovoltaic effect. The photovoltaic effect is the process of creating a voltage in a material by exposing it to electromagnetic radiation such as sunlight or a laser beam.

When photons from sunlight or the laser beam hit a solar panel and are absorbed by semi-conductive materials such as silicon or gallium arsenide (GaAs), they knock electrons loose from atoms creating a positively-charged hole and a negatively-charged electron. The electrons and the holes are repelled by each other due to opposite charges, and the designs of the photovoltaic cells force the electrons to move in a fixed direction creating a current (Frahrenbruch, 1983:9-16) as shown in Figure 3.

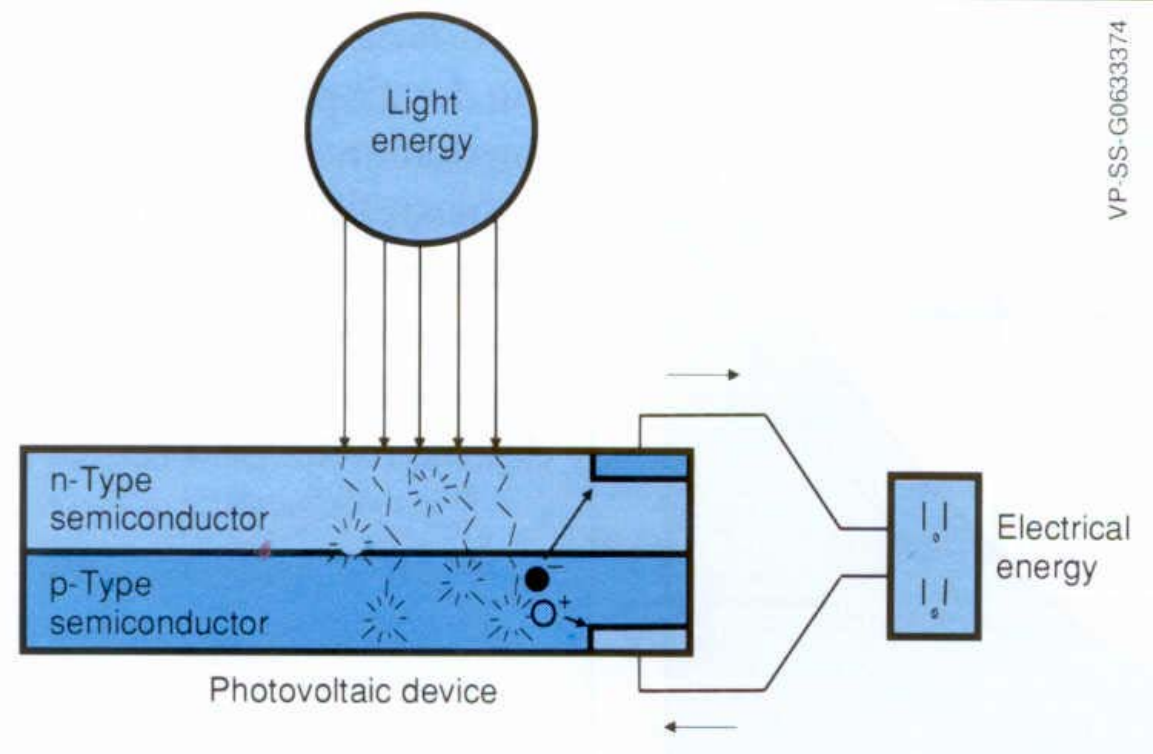

Figure 3: Photovoltaic Effect (Sandia Corporation, 2009)

The n-type semiconductor, shown in Figure 3, is manufactured using atoms capable of providing extra electrons to the host material (Frahrenbruch, 1983:44). The p-type semiconductor provides the extra positively charged carriers (Frahrenbruch, 1983:44). This configuration produces a direct current in the cell that can be used by a load, stored in a battery, or converted to alternating current before use.

The location where the n- and p-type layers of the semiconductor meet is called a junction (Frahrenbruch, 1983:105). Most solar cells only have a single junction, but triple junction solar cells have three junctions, and multi-junction cells have several junctions. Multiple junctions indicate that multiple materials are stacked to for the cells. Junctions between multiple n- type and p-type semiconductors as seen in triple and multi-junction

cells gather light across a larger band of the electromagnetic spectrum which allows them to generate more power with the same incident sunlight. When manufacturing solar cells with multiple junctions, using different materials, it is important to avoid lattice and current mismatches.

A lattice mismatch arises when there is a difference in lattice constants between two junctions. The term lattice is a reference to the crystalline structure of the solar cells coating. When the crystalline structure of two different coatings do not line up perfectly, resulting in dangling bonds, as shown in Figure 4. The effects of dangling bonds can be varied but usually lead to a loss in power (Frahrenbruch, 1983:139).

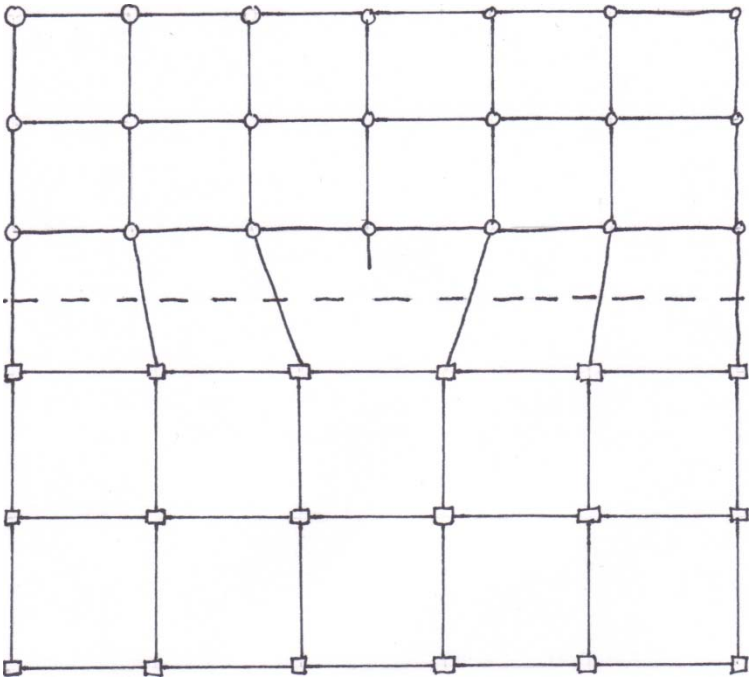

Figure 4: Schematic diagrams of the interfacing of two single cubic crystals with lattice mismatch

Current mismatch is another source of power loss. It is caused by the recombination of electrons and holes at the junction of two materials, and leads to a loss of current (Frahrenbruch, 1983:233). Both current and lattice mismatches can reduce the efficiency of a solar cell.

The primary concern for a photovoltaic cell material in this experiment is their power conversion efficiencies and quantum efficiencies as these two items will determine how much power incident on the spacecraft is converted to usable energy.

2.3.2 Quantum Efficiency

Quantum efficiency determines how much light at a certain wavelength a solar cell is likely to absorb and use to generate power. Therefore the closer a laser's wavelength is to the peak absorption wavelength of a photovoltaic the more efficient the system will be. As each photovoltaic is discussed its quantum efficiency will also be provided.

2.3.3 Power Conversion Efficiencies

Solar cell efficiency is a measure of the amount of power converted for use based on the incident light on the surface of the photovoltaic. Efficiency of cells is usually measured in a lab under standard test conditions (STC): temperature of 25°C, an irradiance of 1000 W/m^2, and an air mass 1.5 (AM1.5) (Space Technology Library, 2008:413).

Current efficiency under these conditions tends to be around 20.8% for Silicon, 21.8% for Gallium Arsenide (GaAs), and 25.7% for Multi-junction Gallium Indium Phosphorous (GaInP)/GaAs (Space Technology Library, 2008:414). However several institutions are currently working on drastically improving these numbers. The U.S. Department of Energy's National Renewable Energy Laboratory announced in 2007 that they had a photovoltaic with a confirmed efficiency of 40.7% under concentrated sun light (Geisz, et al., 2007:2). The University of Delaware working under a DARPA grant has created high-performance crystalline silicon solar cell platform with 42.8% efficiency. A remarkable feat as they do not use a large external collector (University of Delaware Office of Public Relations, 2007) (Barnett, et al., 2006:2564). Meanwhile at the Fraunhofer Institute for Solar Energy Systems ISE located in Frieburg Germany, a multi-junction GaInP/GaInAs/Germanium (Ge) cell has been created that is 41.1% efficient (Guter, et al., 2009:1).

All of these efficiency numbers come from STC which are designed to emulate a sunny day in the northern hemisphere on or around the equinox. Space on the other hand is a vastly different environment which drastically reduces solar cell efficiency. For example the efficiency of Silicon, Gallium Arsenide and Multi-junction cells that have flown in space tend to be 14.8%, 18.5%, and 22% respectively (Space Technology Library, 2008:414).

There are several types of solar cells available today including Silicon, Multi-junction and Vertical Multi-junction solar cells. Each of these is discussed below and each has its advantages and disadvantages.

2.3.4 High Efficiency Multi-junction Solar Cells.

As mentioned above the University of Delaware under a DARPA grant has been performing research on Very High Efficiency Solar Cells. Their lateral solar cell architecture provides a wide range of choices for the materials for multiple junction solar cells.

This flexibility is achieved by avoiding lattice and current matching constraints. It further reduces spectral mismatch losses as the cells have no need to be series connected (Barnett, et al., 2006:2561). By avoiding current matching and lattice constraints the designers allow for the integration of existing high-performance technologies such as Silicon, GaAs, and GaInP into a high performance device (Barnett, et al., 2006:2560). University of Delaware has created GaInP/GaAs tandem cells and is working on Lattice-matched monolithic GaInAsP/GaInAs tandem cells both tuned to 1100nm wavelength (Barnett, et al., 2006:2563).

The fact that they are tuned to 1100nm bandwidth is incredibly important to this experiment as most fiber lasers emit between 1000 and 1100 nm. This close matching will provide excellent quantum efficiency. Multi-junction cells are not the only photovoltaic with high quantum efficiencies past 1000 nm; triple junction cells also offer high quantum efficiencies at these wavelengths.

2.3.5 Triple Junction Solar Cells:

Current state-of-the-art triple junction solar cells make use of a three-junction design that includes a Ge bottom junction which absorbs twice the number of low energy photons than what is required to perform current matching, as shown in Figure 5, as it is not lattice matched with the other junctions made up of $Ga_{0.5}In_{0.5}P$ and GaAs (Geisz, et al., 2007:2).

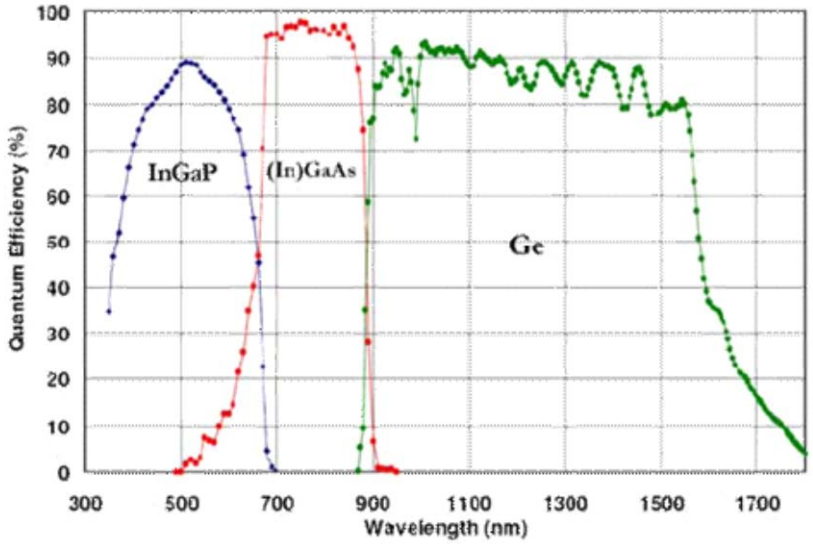

Figure 5: Quantum Efficiency vs. Wavelength in a Triple Junction Solar Cell (Black, 2009)

The Department of Energy has been performing research into replacing the bottom cell with a 1.0 eV junction that is lattice matched with the other junctions (Geisz, et al., 2007:1). The article by Geisz, et al., states that a "structure that combines a metamorphic 1.0 eV $In_{0.3}Ga_{0.7}As$ junction with lattice matched 1.8 eV GaInP and 1.4 eV GaAs junctions" as shown in Figure 6 outperform or rival all reported solar cell

efficiencies for terrestrial and space applications (Geisz, et al., 2007:1). The quantum efficiency for such cells is given in Figure 7.

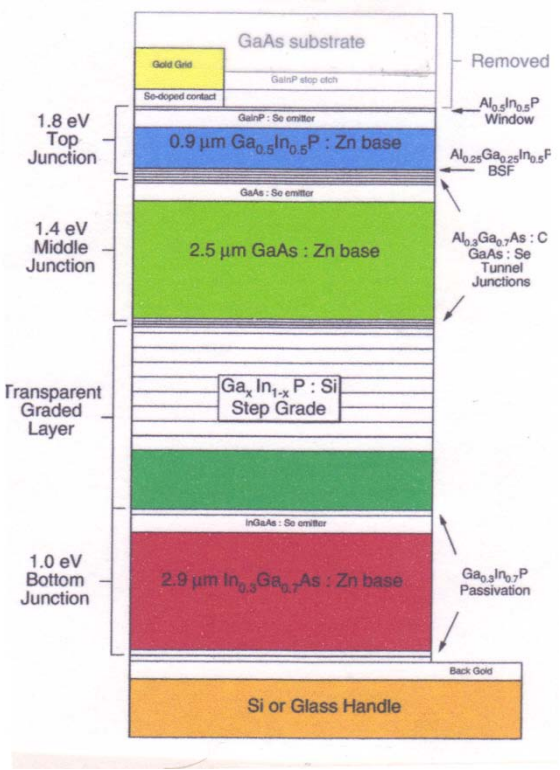

Figure 6: Schematic of inverted triple-junction structure (Solar Energy Technologies Program (U.S.), 2007:20)

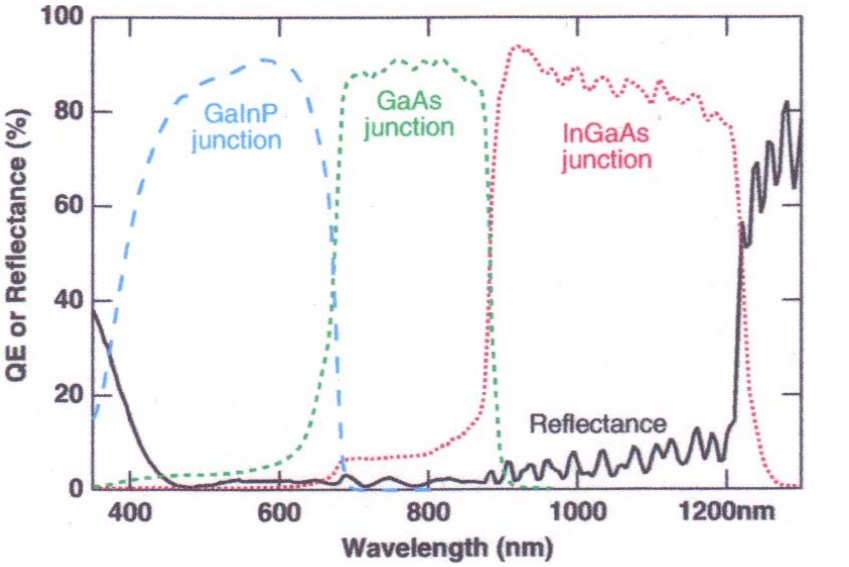

Figure 7: Quantum Efficiency vs. Wavelength in a High Efficiency Triple Junction Solar Cell (Solar Energy Technologies Program (U.S.), 2007:20)

In addition to the boost in efficiency, roughly 10% compared to other triple junction cells, these cells offer the advantage of being lightweight devices that reject unused infrared light, reducing onboard heating (Geisz, et al., 2007:3). In addition to multi-junction and triple junction photovoltaic there is an additional type of junction which may be best-suited for use in the wireless power transfer experiment the experimental Vertical Multi-junction solar cells being developed by PhotoVolt, Inc.

2.3.6 Vertical Multi-Junction Solar Cells

Vertical Multi-junction (VMJ) solar cells are "integrally bonded series-connected array of miniature silicon vertical junction unit cells" designed to operate at extremely high intensities while keeping manufacturing costs low (Sater, 2008:1).

VMJs are well-suited for the collection of high energy intensities of up to 1000 suns. VMJ cells have several advantages over multi-junction cells: Edge illumination is an advantage because it eliminates the need for front or back contact, current instead flows from one cell into its vertical contacts because there is equal probability that currents generated at any depth will be collected. This gives improved spectral responses for both the short and long wavelengths as shown in Figure 8 (Sater, 2008:4).

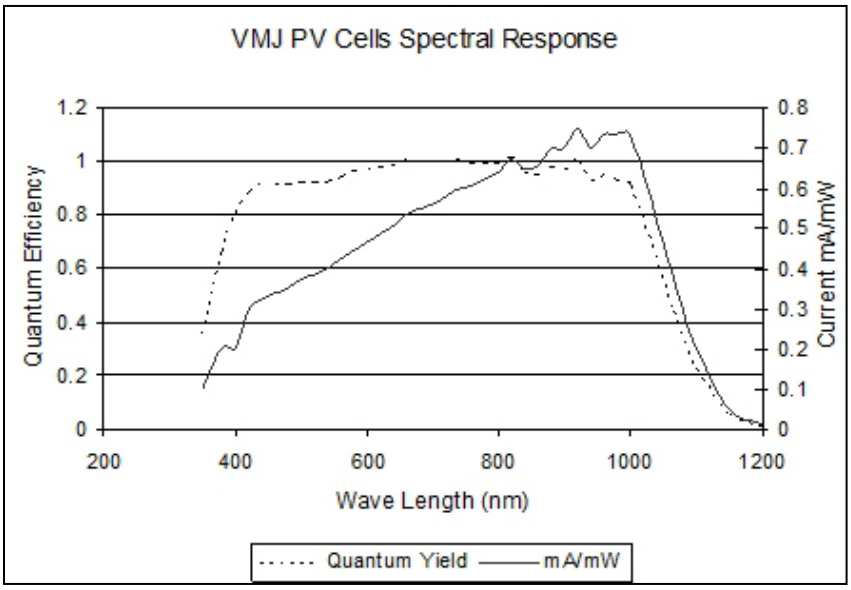

Figure 8: VMJ PV Cells Spectral Response (Sater, 2009)

The series connection provides a high voltage, and low current circuit. To ensure easy compatibility with most power processing loads, it further reduces the need for adding by-pass diode protection because it gives immunity to reversed voltage breakdown. Effective photoconductivity modulation in the bulk region of unit cells provides an almost linear decrease in series resistance. The final advantage listed by B. Sater and N.

Sater is its structural design which provides a rugged configuration electrically, mechanically, and thermally, permitting high packing densities with easy interconnecting of electrical output leads in high power density systems (Sater, 2008:2).

In addition, these cells provided 50% efficiency at the 980 nm wavelength (which is well within the range of wavelength in which high powered chemical lasers operate) in lab tests, making them almost ideally suited for Laser Power Transfer. Several ground-based outdoor experiments have been performed with these cells providing a peak solar flux of 65 W/cm^2 and about 50 W/cm^2 on average due to sun angle, debris, and atmospheric interference (Sater, 2008:2-3).

In the first year of testing there were no indications of voltage or current degradation, but as these cells have never flown in space, radiation-caused degradation testing has not been performed. Considering all of the above these cells appear to be well-suited for the AFIT/NASA experiment. (Sater, 2008:3)

2.3.7 Photovoltaic Concentrators

A photovoltaic concentrating system uses either mirrors or lenses to focus light onto a small area of photovoltaic cells. These systems significantly concentrate sunlight, delivering 500 to 1000 times more than the sun alone (Sater, 2008:1). As solar cells operate more efficiently as you increase the amount of incident light, and since concentrators are significantly cheaper to produce than photovoltaic material, a growing number of photovoltaic systems depend on these types of capabilities to increase their efficiency.

Space systems that use such concentrators require stabilization about one axis with two axis stabilization being preferred in order to keep the concentrator focused on the solar cell and pointed towards the sun. This required stabilization means that a space vehicle with body-mounted solar panels would need to be controlled around at least one axis in order to make use of any type of concentrator technology.

Such a system could be used with the laser power beaming experiment, by incorporating deployable collector/concentrating systems the amount of energy gathered from the laser beam would be increased simultaneously increasing the efficiency of the photovoltaic cells. Alternatively photovoltaic's that incorporate concentrating system could be used to simply increase efficiency.

The University of Delaware's Very High Efficiency Solar Cells discussed above are actually an integrated optical/solar cell design; see Figure 9, which allows efficiency improvements while retaining low overall costs. Furthermore, this design does not require any additional pointing requirements above the solar panel itself (Barnett, et al., 2006:2561). This design not only focuses light onto cells, it also separates light based on wavelength and redirects it optically to cells optimized at a matching wavelengths further improving its efficiency (Barnett, et al., 2006:2561).

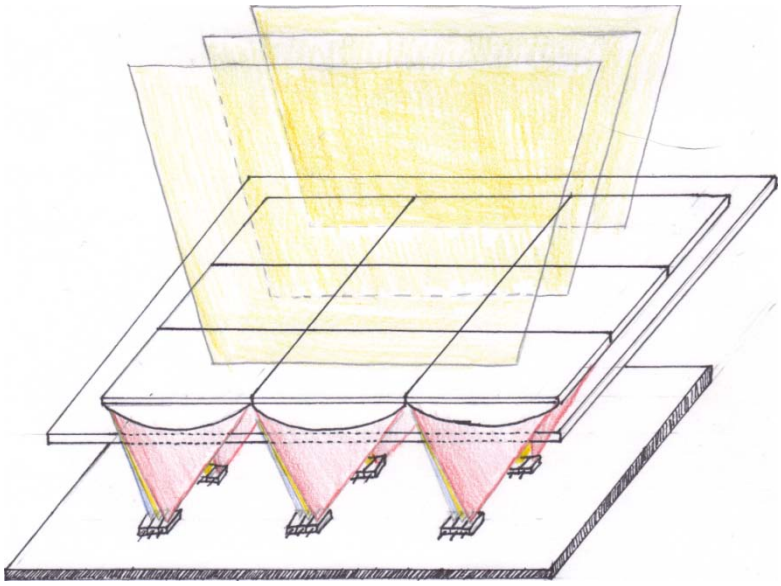

Figure 9: Schematic of the lateral solar cell approach

2.4 Summary

The literature review performed here began with an overview of possible scenarios that could be used to verify the usefulness of the model. It continues by covering the available laser technology in Sect. 2.2.1. The available laser technology makes it clear that an IPG YLR 1000SM is the only commercial off the shelf laser available today which meets all mission requirements. Finally how the satellite might collect the power from the laser system was considered in Sect. 2.4. A summary of each photovoltaic cell type and its applicable characteristics is provided in Table1.

Table1: Solar cell properties (Barnett, et al., 2006:2563) (Geisz, et al., 2007:2) (Guter, et al., 2009:1) (Sater, 2008:3) (Solar Energy Technologies Program (U.S.), 2007:55) (Space Technology Library, 2008:414)

Solar Cell	Achieved efficiency (lab)	QE	nm
Silicon	20.80%	6%	1060
Gallium Arsenide	21.80%	0%	above 900
GaInP/GaAs	25.70%	0%	above 900
Vertical Multi-junction	50.00%	55%	1060
GaInP/GaAs/InGaAs	40.70%	86%	1075
Crystalline Silicon	42.80%	6%	1060
GaInP/GaInAs/Ge	41.10%	90%	1075

With the knowledge of the solar cells available and the selected laser it is now possible to create a model of the power losses the system will face and generate its overall efficiency.

III. Method

This chapter will develop a mathematical model to accurately track the amount of power delivered in a wireless power beaming system. As shown in Figure 10, the power proceeds through several different stages before being delivered to the satellite payload for use. Each of these stage results in additional power losses and are examined below.

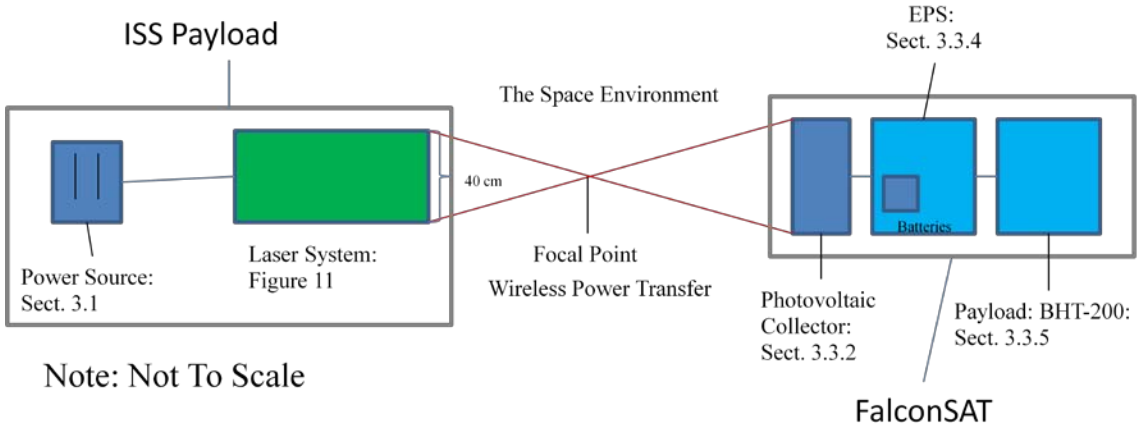

Figure 10: Block Diagram of Wireless Power Transfer

First we will discuss the design of the laser model and the mathematical equations that govern power consumption of the laser system as well as power losses caused by laser system design parameters in Sect. 3.1. Then in Sect. 3.2 we will discuss the impacts of the space environment to the laser beam. Finally in Sect. 3.3 we will model the photovoltaic collector and the losses caused by the EPS system before determining how much power is provided to the payload.

3.1 Method for Designing the Laser

The laser portion of the power beaming experiment is going to be located on the Japanese Experimental Module, Exposed Facility, of the International Space Station (ISS). It will have 3 kW of wall plug power available at 120 volts direct current.

The notional laser system designed by Dr. R. L. Fork of the University of Alabama Huntsville for this project shown in Figure 11 will be used as the baseline laser system in the model. This model will only consider using the IPG YLR 1000SM laser as discussed in Sect. 2.2.4, but it should also be noted that the fast steering mirror has an impact on power delivered as discussed in Sect. 3.1.8, as does the diameter of the primary aperture discussed in Sect. 3.1.3, and Sect. 3.1.4.

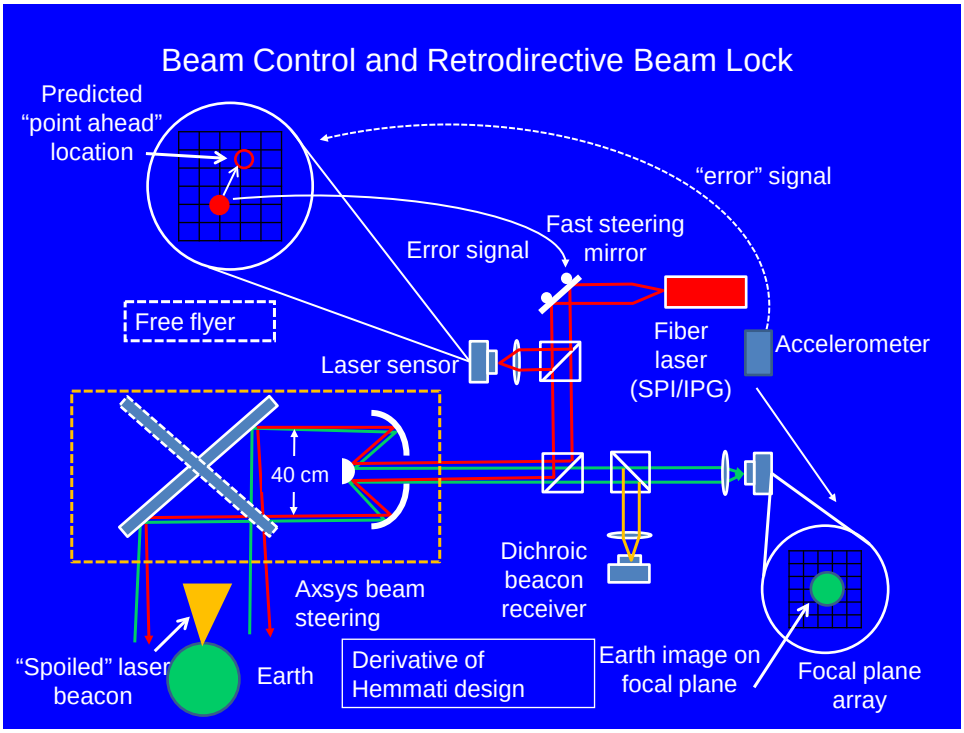

Figure 11: Laser System Block Design (Fork, 2008)

The laser model will calculate basic laser performance to determine the amount of power emitted from the laser based on the amount of wall plug power. The model will then model both the diffraction limited performance, see Sect. 3.1.3, and the Gaussian Performance of the laser, see Sect 3.1.4. By comparing these to results it will be possible to use the model to determine where more controls may be necessary to optimize the amount of power delivered.

Three important factors must be considered when designing the laser. First the wavelength (λ) emitted by the laser, secondly the diameter of the primary aperture (D), shown in Figure 11 to be 40 cm, and finally the efficiency of the laser (η). All three of these system parameters affect irradiance in the far field[3].

3.1.2 Laser Performance Modeling

Initially Equation (1) will be used to determine the power (P_{actual}) output from the laser:

$$P_{actual} = P_{available} * \eta \quad (1)$$

As mentioned above $P_{available}$ is 3 kW and efficiency, η, is 25% as provided in Sect. 2.2.4. Now that we know the amount of power in the beam, P_{actual}, the model will determine the lasers diffraction limited performance.

[3] Irradiance in the far field will equal the amount of irradiance incident on the photovoltaic cell (see Sect. 3.3.2)

3.1.3 Diffraction Limited Performance

Other laser performance factors of interest are radiance, brightness, peak irradiance, beam area, and beam radius. Each of these performance factors will be discussed below as will the method used to determine each within the model.

Radiance (L) as used in laser physics is defined by Equation (2):

$$L = \frac{P_{actual}}{\lambda^2} \tag{2}$$

Radiance is a measurement of intensity and has SI units of Watts per steradian per meter squared (W str^{-1} m^{-2}). It is not to be confused with brightness, as the terms are used interchangeably by other scientific communities.

Brightness (B) in the high energy laser community is a figure of merit that is range independent. Brightness is measured in Watts per steradian (W str^{-1}) and can be found using Equation (3):

$$B = \frac{\pi}{4}\frac{P_{actual}}{\left(\lambda/D\right)^2} \tag{3}$$

The diameter of the primary aperture (D) is the only parameter that can be controlled in the laser design independent of the selection of the laser. As it effects brightness and brightness goes on to effect irradiance, and spot size, as is discussed below, D is a very important design parameter.

The maximum amount of irradiance (I_O), Watts per meter squared (W m^{-2}), at any given range (R) is called the peak irradiance and can be found using Equation (4):

$$I_O = \frac{B}{R^2} \tag{4}$$

Beam area (A_{eff}) is the diffraction-limited amount of area a two dimensional cross section of the laser encompasses in the far field. Beam area can be found using Equation (5):

$$A_{eff} = \frac{P_{actual}}{I} \tag{5}$$

The beam radius, also known as the target waist (w_{O2}), and spot size, is the diffraction-limited far field measurement used to relay the radius of the laser beam at the target. Beam radius is defined using Equation (6):

$$r_d = \sqrt{\frac{A_{eff}}{\pi}} \tag{6}$$

As the laser has near diffraction-limited performance, as discussed in Sect. 2.2.2, the above values give us a good understanding of the laser's optimal performance. However, a better understanding of how the laser will function in an operational environment can be gained by using a Gaussian beam model to account for additional loses the laser may experience.

3.1.4 Gaussian Beam Propagation

As a laser propagates through space, it changes size just as a spot of light from a flashlight gets bigger as you move further away from the target. As the spot size

increases, the amount of power in the beam remains the same; therefore the amount of power incident per unit area decreases. At extreme distances there may not be enough power in any one segment of the spot to power the target satellite. For this reason it is important to understand how the spot size changes with distance and what can both positively and negatively impact the change along the way.

Although there are numerous ways to model this change, a Gaussian Performance Model will be used here, and a single mode Gaussian laser is used in the model. Single mode operation is a condition in which an optical wave does not exceed the minimum value for the occurrence of the next higher mode; in essence there is only one wavelength that can successfully propagate inside the laser cavity (See Sect. 2.2.2). It can be effectively modeled as a Gaussian because:

> The lowest-order mode of the cylindrical step-index fiber has a bell shaped profile resembling the transverse envelope of the Gaussian TEM_{00} mode in homogenous medium. Therefore a free-space Gaussian beam can be efficiently coupled to the ground mode of a single-mode fiber (Meschede, 2007:46).

This bell shaped profile is similar to the one shown in Figure 12.

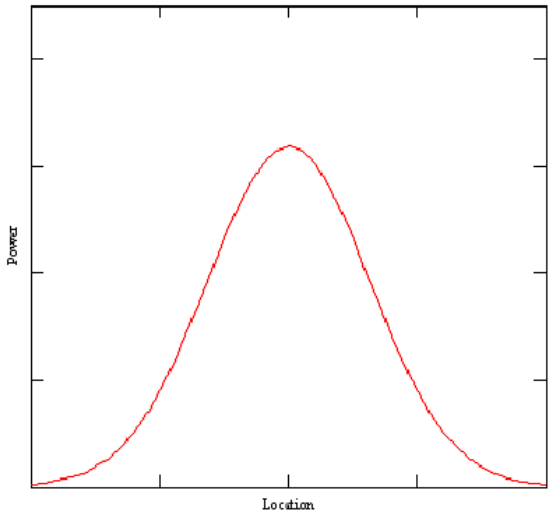

Figure 12: Typical Gaussian Shape

As with all performance models, the Gaussian performance model can be considered an interpolation function within the given performance space of the wireless power transfer system (Cusumano, 2008). The Gaussian model is particularly useful because not only does it model everything that can impact a laser, such as jitter or the atmosphere, it can be easily molded to only account for impacts that are expected. For example the atmosphere will not be an important factor as its density is effectively zero, as shown in Sect. 3.2.1. At the ISS orbital altitude the experiment is in a vacuum. The atmosphere component is therefore removed from the model. This approach leaves room for expanding the model in the future if we desired to determine the effectiveness of the laser in delivering power to a ground station from orbit as in Case Study 1 in Sect. 4.3.

The overall power beaming system model developed here will use Gaussian Performance modeling to determine the far field spot size, and the impact of the JEM/EF

vibration, also known as platform jitter. These results will be compared to the diffraction-limited results, where applicable, in order to determine if additional controls are required for the laser system to minimize losses.

3.1.5 Determining Spot Size

The target waist can be determined using Equation (7):

$$\frac{1}{w_{O2}^2} = \frac{1}{w_{O1}^2}\left(1 - \frac{z_1}{f}\right)^2 + \left(\frac{\pi w_{O1}}{f\lambda}\right)^2 \tag{7}$$

where w_{O2} is the target waist (in meters), w_{O1} is the initial waist; f is the focal length of the primary aperture, and z_1 is the Rayleigh range the distance over which the beam area increases by a factor of two (Perram, 2009).

It will be assumed that the focal length is approximately equal to the range of the target as this design greatly reduces losses. The initial waist is the same as the radius of the primary aperture ($D/2$), and that z_1 is much smaller than f. This allows Equation (7) to be reduced as shown below:

$$\frac{1}{w_{O2}^2} = \frac{1}{\left(D/2\right)^2}\left(1 - \frac{z_1}{R}\right)^2 + \left(\frac{\pi D/2}{R\lambda}\right)^2 \tag{8}$$

$$\frac{1}{w_{O2}^2} = \frac{4}{D^2}(1-0)^2 + \left(\frac{\pi D}{2R\lambda}\right)^2 \tag{9}$$

$$\frac{1}{w_{O2}^2} = \frac{4}{D^2} + \left(\frac{\pi D}{2R\lambda}\right)^2 \tag{10}$$

where D is the diameter of the primary aperture, λ the wavelength of the laser, R is the range and w_{O2} is the target waist. Not only is Equation (10) less complicated than Equation (7) it is also made up of components that we designate with the design of the laser and therefore will be used to find w_{O2}.

3.1.6 Gaussian Irradiance

Once the spot size is known we can use it to determine irradiance from the Gaussian model as shown in Equation (11):

$$I = \frac{P_{actual}}{\pi w_{O2}^2} \tag{11}$$

where I the irradiance in the far field, w_{O2} is the target waist or spot size of the laser in the far field and P_{actual} is the power emitted from the laser.

3.1.7 Strehl

Up until this point the model has assumed that only the size of the laser beam will change and that the amount of power in the beam (P_{actual}) will remain constant. This assumption is not actually the case. In reality a laser beam will suffer from degradation caused by outside sources as it propagates. The amount of power actually received by the target is compared to the diffraction limited performance discussed in Sect. 3.1.3 in order to determine a Strehl ratio (Cusumano, 2008).

A Strehl ratio is a number between 0 and 1, a Strehl of 0.8 is considered to be outstanding in the high energy laser community (Cusumano, 2008). For example if the diffraction limited maximum intensity for the laser was 260 W/m^2 but the intensity delivered to the target satellite was only 210 W/m^2, then the Strehl ratio of the system would be 0.8.

Sources of Strehl include, but are not limited to thermal blooming, atmospheric absorption, and platform jitter. As the ISS is assumed to be in vacuum the only sources of degradation for which the model needs to account for are caused by platform vibration called jitter, the correction of the fast steering mirror, and the central obscuration created by the use of a secondary mirror, shown in Figure 11, as all others are considered atmospheric effects. The affects of Strehl on irradiance for the above example is shown in Figure 13.

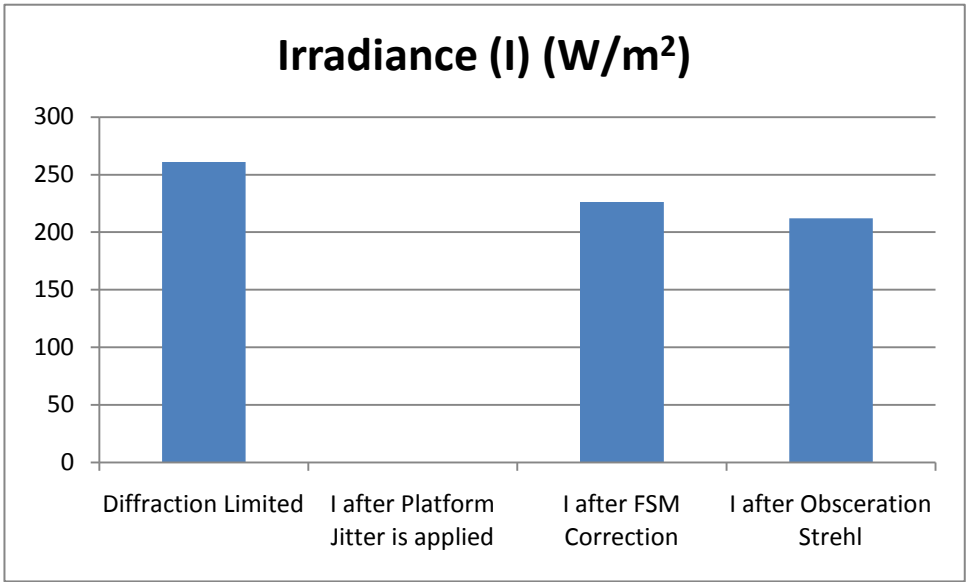

Figure 13: The affects of Strehl on Irradiance

3.1.8 Strehl due to Platform Jitter

Strehl caused by jitter is the degradation of the beam intensity caused by the movement of the platform on which the laser is mounted on. In the case of this experiment it is defined by the vibration of the JEM-EF which has jitter (θ_j) shown in Figure 14. Plugging this value into Equation (12) allows the model to converts this value to a Gaussian shape σ_j:

$$\sigma_j = \frac{\theta_j}{\lambda/D} \tag{12}$$

> This is another reason for using a Gaussian shape. If we have a Gaussian beam and Gaussian jitter, the variance of the jittered beam is simply the addition of the variance of the beam shape and the variance of the jitter (Cusumano, 2008).

The model can then use the ratio of the diffraction limited beam area to the actual beam area to solve for the Strehl due to jitter in a Gaussian form as shown in Equation (13):

$$S_p = \frac{1}{1+\frac{\pi^2}{2}\left(\frac{\sigma_j^2}{\lambda/D}\right)} \tag{13}$$

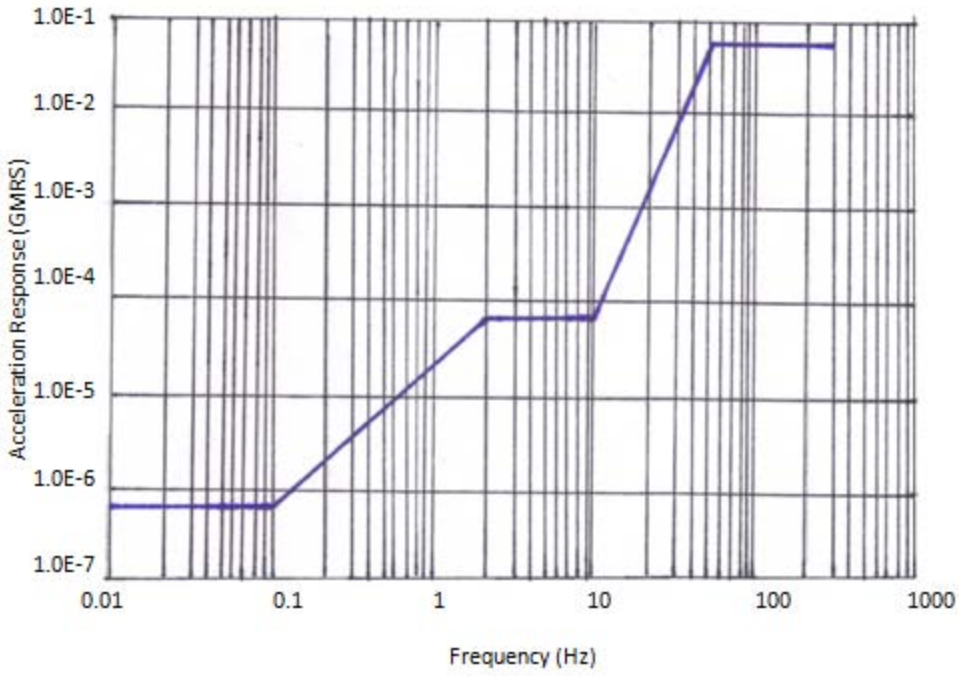

Figure 14: The vibration environment of the ISS

3.1.10 Compensating for Strehl with a Fast Steering Mirror

A fast steering mirror (FSM) is the device used to create line of sight stability. The fast steering mirror corrects error induced by jitter by responding to the movement of the platform in order to keep the laser beam steady, which in turn reduces the amount of Strehl caused by jitter reducing the losses in the system. Typically a fast steering mirror will have an angular range of greater than one milliradians. Other typical values for fast steering mirrors can be found in Table 2 (Cusumano, 2008).

Table 2: FSM Typical Values (Cusumano, 2008)

Weight	<200lbs
Tilt Range	+/- 1 mrads
Angular Acceleration	2,000-6,000 rad/s^2
Quiescent Jitter	<0.001 mrad
Caged Bandwidth	800 Hz
Gain Margin	10 – 15 db
Phase Margin	45 - 55 degrees
Residual Reaction	1%
Power Consumption	100 – 150 W

Fast steering mirrors correct for Strehl due to platform jitter but are not perfect. For this reason the model must account for additional Strehl caused by the fast steering mirror. The Strehl caused by the fast steering mirror is shown mathematically in the model using Equation (14) and Equation (15):

$$\sigma_{FSM} = \frac{\theta_{FSM}}{\lambda/D} \tag{14}$$

$$S_{FSM} = e^{-\sigma_{FSM}^2} \tag{15}$$

3.1.11 Strehl due to Obscuration

The telescope, shown in Figure 11, also induces Strehl in the system as it obscures some of the primary aperture from receiving illumination by the laser. This can be accounted for using Equation (16):

$$S_{obs} = (1 - \varepsilon^2) \tag{16}$$

Where ε is the obscuration ratio measured as a ratio of linear distances (Cusumano, 2008), for our system the diameter of the secondary aperture is assumed to produce a 10 cm diameter obscuration and the primary aperture, shown in Figure 11, has a 40 cm diameter, so: $\varepsilon = 0.25$.

3.1.12 Accounting for Strehl in the Model

To determine the peak irradiance delivered by the laser system and incident on the solar panel, or the effect of Strehl, simply take the dot products of Equation (12), Equation (13), and Equation (15) discussed in Sections 3.1.8 and Sect. 3.1.10 with the solution to the initial irradiance given by Equation (11) as shown in Equation (18).

$$\mathrm{I_{peak}} = \mathrm{I_O} * \mathrm{S_P} * \mathrm{S_{obs}} * \mathrm{S_{FSM}} \tag{17}$$

Once the peak irradiance is known it can be applied to the target satellite as covered in Sect.3.3, but first it is important to ensure that all environmental affects have been accounted for.

3.1.13 Safety Factors

Laser beams can generate considerable heat. This leads to concern that the receiving satellite or potentially a third party satellite could be damaged by the intensity of the beam. For this reason the model will perform a lethal fluence check in order to

ensure that the irradiance of the beam will not damage the receiving satellite.[4] As the fluence is low enough not to harm the receiving satellite it will pose little threat to the structure of any third party satellite which passes through the beam.

3.2 Modeling Environmental Losses

Several environmental factors need to be considered to ensure that any losses caused by the environment are accounted for. Careful consideration of the environment in which the wireless power transfer experiment will take place is required in order to ensure the model accounts for all environmental degradation. As mentioned before and shown below the model can disregard atmospheric impacts as the experiment takes place in a vacuum; however, the model must also account for the effects of daylight, range to the receiving satellite and contact time as discussed in Sect 3.2.2, 3.2.3.

3.2.1 The Atmosphere

Sect. 3.1.4 states that the experiment takes place on board the ISS which is located in a vacuum. The ISS is actually located in the upper thermosphere; at an altitude of 336 km (perigee), as is shown below it is still safe to assume that the experiment takes place in a vacuum but the atmosphere does impact the mission. The ISS is specifically located in the F2 region of the ionosphere. The thermosphere has the highest kinetic temperature in the atmosphere, and the temperature varies dramatically with solar cycle

[4] As fluence is combination of range and contact time each contact should be checked individually

as the heating is caused by absorption of short wavelength photons which appear in greater number during solar max. This temperature variation will be an important facture in acquiring the satellite, as the thermosphere increases in temperature it expands, effectively increasing the amount of drag experienced by low earth orbiting (LEO) satellites slowing them down. A LEO satellite may not be where its two line element set predicts because of a drag induced change in velocity; please see Appendix A for more information.

This region of the atmosphere is dominated by monatomic Oxygen with some N_2 also present. These constituents are separated by mass, and spread out considerably. The density of the thermosphere can be calculated using Equation (18):

$$n(z) = n(z_0) * \exp\left(-\frac{z-z_0}{H}\right) \tag{18}$$

Where z is altitude, $n(z_0)$ is the starting density of the oxygen, and H is given by Equation (19):

$$H = \frac{kT}{mg} \tag{19}$$

Where k is Boltzmann's constant, T is the temperature (1200 K), m is the mass of oxygen, and g is the acceleration of gravity. To determine the density of the thermosphere first calculate H, for oxygen, using the known physical quantities at the altitude of the ISS in order to solve for the scale height of $1.05558x10^{-22} kg\ s^2$, or approximately zero.

Placing *H* into Equation (18) quickly reduces the exponent to negative infinity which solves for an atmospheric density of zero. Mathematically then it is clearly reasonable to model the transfer of power as if it were taking place in a vacuum. Therefore the Gaussian model will assume no atmospheric effects or losses just as if the experiment was taking place in a true vacuum.

3.2.2 Eclipse vs. daylight

As will be shown in Sect.3.3.4, the efficiency of the electrical power subsystem varies with sunlight. Since satellites tend to be about 10% more efficient during daylight, the model should show greater power delivery to the Hall Effect Thruster during power transfers that occur during daylight over those that occur during eclipse. In the model, a simple true/false input will determine when the satellite is eclipsed.

3.2.3 Range

In order to determine the effective range of the power transfer, it is necessary to use the satellite model to determine the minimum amount of irradiance that must be delivered to power the payload. FalconSAT 5s payload is a Busek Hall-Effect Thruster (BHT-200) an identical payload will be assumed to be present on board the receiving satellite, see Sect. 3.3.5, and the laser will need to deliver enough power for the satellite to fire the BHT-200. To perform this function the satellite requires about 106 W/m^2 of irradiance from the laser. Once the model has determined the required irradiance (***I***) it can be plugged into Equation (20) in order to solve for *R* in Equation (21):

$$I = \frac{P_{actual}}{\pi w_O^2} \tag{20}$$

$$w_O = \frac{R\lambda}{\pi(D/2)} \tag{21}$$

Where P_{actual} is the power output of the laser, D is the diameter of the primary aperture, λ is the wavelength of the laser, and w_O is the target radius at range R. This calculation gives the baseline model an effective range of approximately 880 kilometers.

3.2.4 Contact Time

For the purpose of this experiment, contact time is defined as the amount of time the satellite spends within the effective range and unobstructed view of the laser. This will be determined using a Satellite Tool Kit (STK) v9.0.1™ model. Tracking all possible objects that might block the laser's view of the satellite, the determination of appropriate look angles, along with optimizing its orbit to maximize contact time are the subject of *Mission Analysis and Design for Space Based Inter-satellite Laser Power Beaming*, a research thesis being performed in parallel to this work. For this reason the model will use the orbital design for FalconSAT 5 to determine contact time but it is expected that this will result in less power than the amount transferred with the optimized orbit.

3.3 Method for Building the Satellite Model

As the proposal for the NASA experiment was to use a small satellite as the target for the laser power beaming experiment and because FalconSAT 5 has $15 million of development already in place along with the flight heritage it will have experienced by the time the wireless power transfer experiment launches, the baseline satellite model will be a replica of FalconSAT 5 which already uses a Busek Hall-effect thruster. This model will be modified by to minimize the amount of power lost within the satellite while still maintaining as much of the original design as possible to reduce the costs of developing the target satellite.

It is necessary to model how the power will be collected, Sect. 3.3.1, how the Electronic Power Subsystem will manage the power, Sect. 3.3.2. Furthermore how much power is required by the payload will be required as an input so that the model can be used for other missions, Sect 3.3.3. Finally the any power storage method used will be modeled as described in Sect 3.3.4 to allow the model to be used for missions that desire to store the power to be used by a payload at a later date.

3.3.1 Modeling the Collector

For the initial model it will be assumed that a photovoltaic collector identical to the one flown on FalconSAT 5 will be used. By varying the size and type of collector, the model will show the effect on total power absorbed from the laser.

FalconSAT 5 makes use of four solar panels, each 20.25” x 19.2”, and made up of triple junction Gallium Arsenide solar cells. These solar panels are placed on the satellite

as shown in Figure 15 with a single solar panel on each side of the satellite. For this reason it is assumed that only one panel will be illuminated at a time.

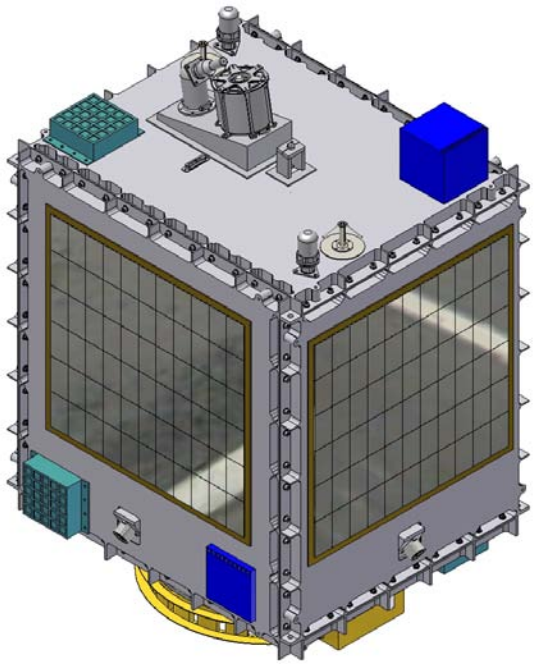

Figure 15: FalconSAT 5 showing one Solar Array for each side panel (Space Systems Research Center, 2007:4)

The irradiance (I) of the laser on the solar panel is known from Equation (18) and the efficiency (η) of each type of solar cell considered is documented in Table1 in Sect. 2.5. This table allows the model to calculate the output power (P_o) of the solar array by using Equation (22) (Space Technology Library, 2008:413):

$$P_O = \eta \text{ x } I \tag{22}$$

Once the output power (P_O) is known, it can be used to determine the amount of power required from the solar array at the beginning of the satellite‘s life. The model determines the amount of beginning of life power by solving Equation (23):

$$P_{BOL} = P_O I_d \cos\theta \tag{23}$$

Where θ is the angle of incidence with which the laser strikes the solar array, initially it will be set to 45^o, but can be varied to account for changes in the satellites attitude. I_d is the nominal inherent degradation of the solar cell, considered to be 0.77 (Space Systems Research Center, 2007:81) (Space Technology Library, 2008:412).

In order to determine how much power must be produced by the solar panel at the end of the mission life, the results of Equation (23) and Equation (24) can be placed into Equation (25) to solve for the required end of life power (P_{EOL}):

$$L_d = \left(1 - \frac{\text{degradation}}{\text{year}}\right)^{\text{satellite life}} \tag{24}$$

$$P_{EOL} = P_{BOL} L_d \tag{25}$$

Where L_d is the lifetime degradation of the photovoltaic over the lifetime of the satellite, which in the case of FalconSAT 5 is one to three years (Space Systems Research Center, 2007:44), the degradation per year experienced by gallium-arsenide cells in LEO is about 2.75%, and the degradation per year silicon cells experience is roughly 3.75% (Space Technology Library, 2008:413), as both types of cells will be considered by the model it is important that the correct degradation value is input into constraint space.

With the end of life power (P_{EOL}) known, it is now possible for the model to find the required power output of the solar array (P_{sa}) by rearranging Equation (26) to solve for the power provided by the solar array (P_{sa}) as shown in Equation (27):

$$A_{sa} = \frac{P_{sa}}{P_{EOL}} \tag{26}$$

$$P_{sa} = P_{EOL} A_{sa} \tag{27}$$

The model of the solar array will begin at a fixed size equal to the solar array area (A_{sa}) on board FalconSAT 5. Therefore A_{sa}=20.25" x 19.2" (Space Systems Research Center, 2007:81). The area of the solar cells will be an input to the model so that the area can be changed as the model is used to explore different case studies.

3.3.2 Modeling Losses Inherent in Electronic Power Subsystem (EPS)

The standard method used to determine power required from the power source when using photovoltaic's is given by Equation (28):

$$P_{sa} = \frac{\left(\frac{P_e T_e}{X_e} + \frac{P_d T_d}{X_d}\right)}{T_d} \tag{28}$$

Where P_d is the power required when the space vehicle is in sunlight, T_d is the amount of time the satellite is in sunlight, X_d is the efficiency of the spacecraft while in sunlight, and P_e T_e and X_e represent the power required, the length of time, and the efficiency of the satellite in eclipse respectfully. However, in the NASA experiment the Sun is not the

power source; a laser on board the ISS is. The efficiency differences between eclipse and daylight will still effect the power collection and consumption, as the temperature change directly impacts the efficiency of EPS systems. Therefore Equation (28) needs to be modified slightly to appropriately model the losses caused by the EPS system.

The numerator of Equation (28) calculates the power consumption, where as the denominator is the amount of time available each orbit for charging. For ease of calculation it is assumed the thruster will be fired no more than once for each pass of the space station. This allows for the replacement of P_e and P_d by the amount of power required by the Hall Effect Thruster (P). The equation can then be split into two separate equations. The first Equation (29) calculates the power required if the thruster is fired while the satellite is in eclipse:

$$P_{sa} = \frac{\frac{P * T_t}{X_e}}{T_r} \tag{29}$$

Where T_t represents the amount of time the thruster will be turned on, and T_r indicates the time the target is within range of the laser to receive power.

The Second Equation (30) demonstrates the power required if the thruster is fired while the satellite is in daylight:

$$P_{sa} = \frac{\frac{P * T_t}{X_d}}{T_r} \tag{30}$$

Since X_e and X_d are determined by the power regulation scheme, see Sect. 3.4.2, used by the satellite substituting in the known value of P_{sa} and rearranging the above

equations to solve for *P* allows the model to account for power losses caused by on board EPS inefficiencies.

3.3.3 Modeling the Hall Thruster

The power load for this experiment is assumed to be a Busek Co. BHT-200™ Hall Effect thruster on board the target satellite. According to the Busek pamphlet at 200 Watts the *Propellant Mass Flow rate is* 0.94 mg/sec, and the *Specific Impulse is* 1390 sec, yielding a thrust of 12.8 mN. Therefore these values will be used as the baseline values for the thruster. The work by the U.S. Air Force Academy on FalconSAT 5 shows that this thruster's input power can vary from 50 to 750 W for this reason 50 to 750 W will be used as the acceptable range of power for the system load.

3.3.4 Modeling Power Storage

The power storage subsystem on board must be able to store enough energy to fire the thruster when the satellite is not in range of the ISS and therefore cannot be powered by the laser. In order to select a power storage system, it was first necessary to determine how frequently the thruster would need to be fired when the ISS was not in view, and the total amount of power required for such a maneuver. It is assumed that only one thruster firing will occur for each pass of the ISS and that the amount of power required is predetermined, see Sect. 3.3.5.

For the baseline model, Sony Nickel Cadmium (Ni-Cd) batteries, with 90% transmission efficiency (Space Systems Research Center, 2007:82), will be used. Nickel

Hydrogen (NiH_2) will also be considered. Both of these batteries are space qualified and have a performance record proving they are adequate for the mission (Space Technology Library, 2008:420).

The transmission efficiency measures how much of the power sent to a battery is stored and ultimately available for use by a power load. For this reason it is always more efficient for a load such as a thruster to get its power directly from the primary power source than the on board batteries. This transmission efficiency will lead to more power loss and a less efficient system when the Hall Effect Thruster is used outside of the effective range of the laser.

The model will need to aid in the selection of the most efficient battery type and then calculate the amount of battery capacity (C_r) required for each possible satellite design using Equation (31):

$$C_r = \frac{P_e T_e}{(DoD)Nn} \text{ W-hr} \tag{31}$$

where *DoD* is the depth of discharge expected in low earth orbit, typically less than 20% (Space Technology Library, 2008:420), *N* is the number of batteries on board, and *n* is the transmission efficiency between the battery and the load, finally P_e and T_e as previously defined in Sect 3.3.4. This number can also be divided by the bus voltage to produce an answer in Amp-hr.

3.4 Design Points

In the process of modeling the satellite a handful of critical design drivers have become apparent. The first is what type of photovoltaic cell is used is a system level design consideration as the efficiency relies on the selection of the laser as well, see Sect 3.4.1. The power management model used by the satellite be it Peak Power Tracking or Direct Energy Transfer is evaluated in Sect. 3.4.3 because it directly effects the efficiency of the power transfer from the collector to the load. Finally a handful of critical design points can be found in the laser system as discussed in Sect. 3.4.4.

3.4.1 System Design Points

The first critical system design point is the type of photovoltaic, and the type of laser used. These design choices are interrelated, each affecting the other. The laser drives the efficiencies of the power gathering sources both by the irradiance experienced by the satellite, and the wavelength at which the laser beam radiates the space vehicle.

3.4.2 Solar Cell Options

A number of already existing and experimental solar cells are available for the satellite used in the wireless power transfer experiment. Which one is used will be determined by finding the most efficient solar cell laser combination. This combination matters because each laser emits at a single wavelength or very narrow wavelength band, and quantum efficiency of photovoltaic cells vary with the wavelength of light as shown in Figure 5, Figure 7, and Figure 8. The quantum efficiency (*QE*) value at the lasers

wavelength will be multiplied into Equation (18) to determine the final irradiance on the solar cell for Equation (23). This is shown in Equation (32):

$$\mathrm{I} = \mathrm{I}_{\mathrm{peak}} * \mathrm{QE} \tag{32}$$

3.4.3 Satellite Design Points

X_e and X_d used in Equation (29) and Equation (30) differ for different power management schemes used by the electric power subsystem. As they represent the efficiency of the EPS component of the model it is important that they be as high as possible. The two power regulation schemes considered here are Peak Power Tracking (PPT) currently used by FalconSAT 5, and the more efficient Direct Energy Transfer (DET). PPT give a value of 60% during eclipse (X_e) and 80% during daylight (X_d) whereas with DET X_e is 65% and X_d is 85%.

3.4.4 Laser Design Points

Three major design drivers for the laser are evident. The first, the selection of the laser is addressed in Sect. 2.2.4. From this section it is clear that the IPG Photonics YLR 1000SM is the only known laser on the market today that meets mission requirements. The second design point is the fast steering mirror (FSM). The important aspect of the fast steering mirror is the response frequency with which it responds to the platform jitter as discussed above in Sect. 3.1.11. The third design point is the primary aperture. As the design of the laser is being performed by the University of Alabama Huntsville, the

system level model will assume a FSM keeping with the capabilities shown in Table 2 as well as a primary aperture diameter of 40 cm as shown in Figure 11.

3.5 Summary

Now the model has been designed it is important to validate and verify that the model is functioning correctly so that users of the model can have confidence in its results. Such an analysis is performed in Chapter V.

IV. Analysis and Results

An analysis of the model is provided below, full validation and verification is performed. The analysis will validate the model by ensuring that the model correctly predicts the amount of power transferred, and verify the model by ensuring it accounts for each and every loss that the system is likely to experience. It will do this by using software to test individual equations and the model as a whole to ensure that it is functioning as expected.

4.1 Test Software

In order to perform the analysis outlined in Sect. 4.2-Sect. 4.4, MATHCAD 14^{TM}, and Phoenix Integrations Model Center 8.0^{TM}, where required. Model Center was used to vary the inputs to the equations in the MATHCAD model and graph the output as outlined below. Furthermore Model Center allowed the results of the complementary work *Mission Analysis and Design for Space Based Inter-satellite Laser Power Beaming* which developed an STK model (Keller, 2010:Chap III) to be used to automatically plug in the range and contact time values in the model.

4.2 Laser Component Analysis

To validate that the laser meets mission requirements, parametric studies where performed to evaluate the power output, brightness, and irradiance of the laser, using the following constraints: the laser only accepts power (P) up to the 3 kW available, with

25% efficiency, as defined by the laser selected (IPG Photonics Corporation, 2009a:4) and λ will be between 1060 and 1080 nm (IPG Photonics Corporation, 2009a:4), in order to verify that the laser works as intended key variables in the component where altered in a predictable manner and the output of the model compared with expected results.

The first and most simplified check that the model is working correctly was to validate that as wall plug power increases so did power output or P_{actual} as expected from Equation (1).

As discussed in Sect. 3.1.3 brightness is the range independent figure of merit for the laser it most accurately reflects the effectiveness of the laser design for this model. It was verified, as was expected from Equation (3), that as power (P) increases linearly the brightness of the laser will also increase linearly.

The peak irradiance in the far field can also be linked back to the wall plug power of the laser as demonstrated in Sect. 3.1.3. For this reason it was verified that if you hold all other variables constant and increase power from 0 to 3 kW you will see a corresponding increase in irradiance.

The largest impact to far field irradiance will be the range to the target. To ensure that the model accounts correctly for this, range was varied from 10 km to 880 km while all other variables where held constant. As expected the amount of irradiance available in the far field drops off quickly as range increases. The results of this test are shown in Figure 16 where range exponentially decreases as range increases.

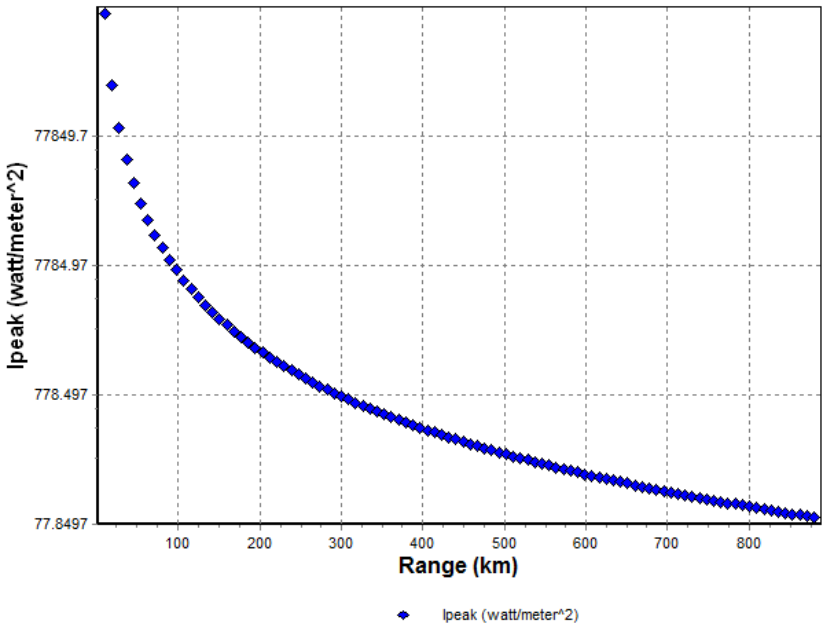

Figure 16: The Impact of Range on far field irradiance (I_{peak})

The primary cause of this decreased irradiance is an increase in the spot size of the laser, therefore it is expected that as this range increases the effective area will also increase causing the corresponding drop in power. This is shown in Figure 17.

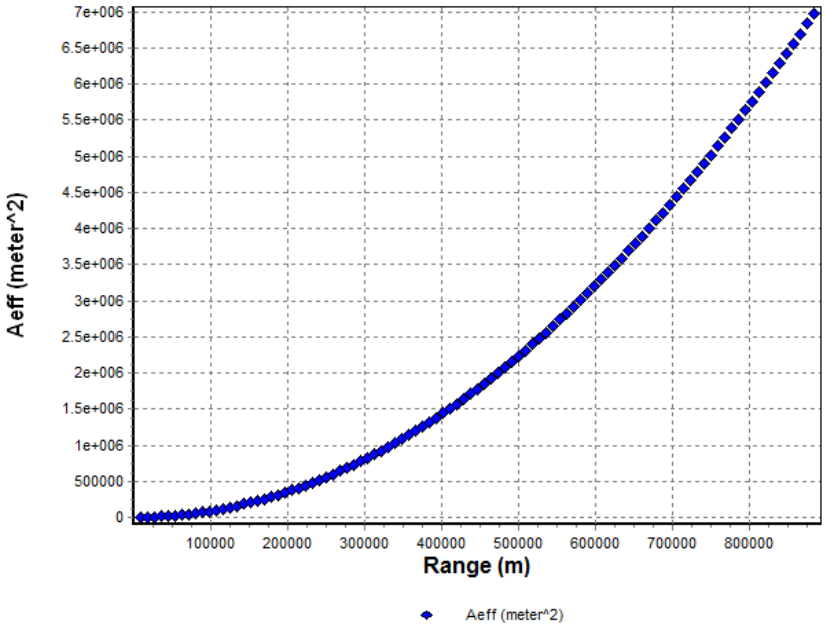

Figure 17: Laser A_{eff} (spot size) range induced growth

The analysis of the laser component demonstrates that the output of the laser model can be trusted. Similar analysis of the EPS component is also required to ensure that the system model is can be verified.

4.3 Satellite EPS Component Analysis

To validate that the EPS model of the satellite is working correctly, several tests were performed. First each of the photovoltaic relevant efficiencies, quantum efficiency, and photovoltaic power conversion efficiency, were run with values ranging from 0% to 100% with 1% intervals. As expected the linear increase in efficiency also increases total time (T_t) the payload can operate, and total power (P_t) available linearly.

As discussed in Sect. 3.4.3 PPT and DET make a difference on how much power makes it through the system to the thruster. As shown in Figure 18, for the same amount of power delivered to the satellite a DET system, allows the thruster to fire longer than a PPT system.

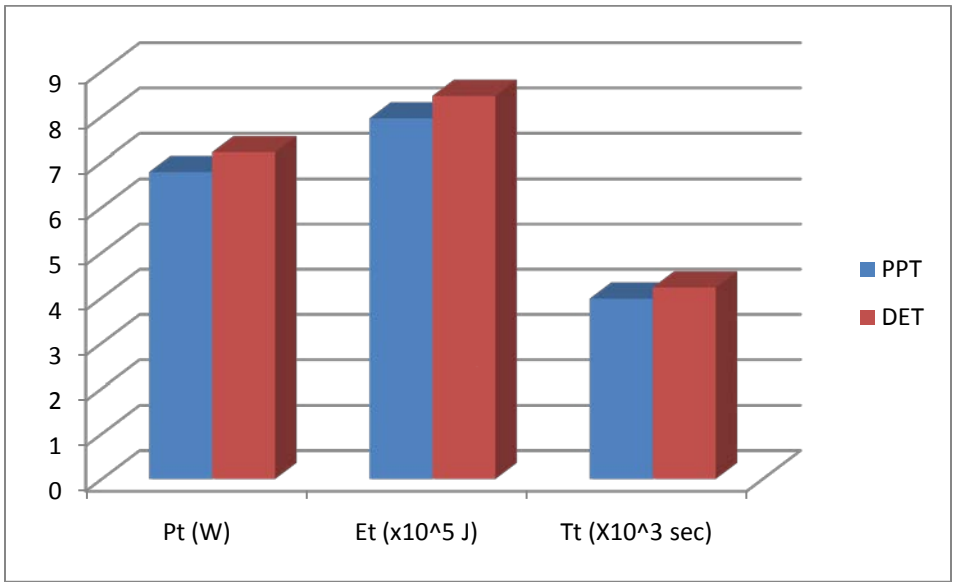

Figure 18: The amount of power/energy transferred and length in seconds the thruster can fire

Figure 18 shows the benefits to having the satellite use a DET power model over the baseline PPT power model; it results in a 6% increase in the amount of time a payload can operate. This satellite component analysis demonstrates that the model is performing as expected and allows for the verification of the wireless laser power beaming system.

4.4 System Level Analysis

To validate that the integrated model of the entire laser power beaming experiment functions correctly, system level analysis was performed. Power flow was modeled to observe the impact on total energy delivered (E_t) as wall plug power, the diameter of the primary aperture, the size of the secondary aperture, and the effectiveness of the fast steering mirror were varied.

As before wall plug power was varied from 0 to 3 kW. The primary aperture was varied from 10 to 150 cm. As expected the linear increase in wall plug power led to a linear increase in the power delivered. The impact of varying the primary apertures diameter can be seen in Figure 19.

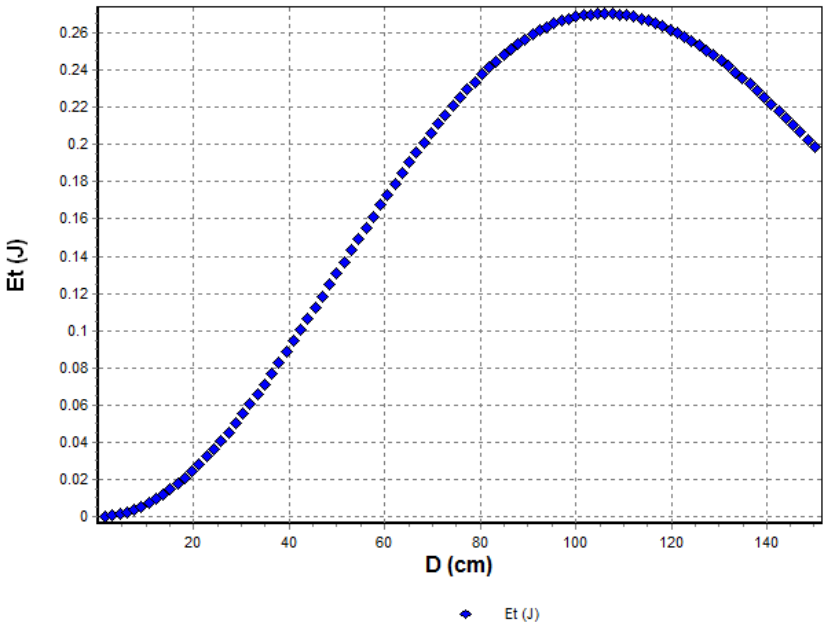

Figure 19: Total energy delivered vs. size of primary aperture

Figure 19 for the first time provides evidence that things don't always get better as they get bigger. The results however are accurate. Careful examination of Equation (10) reveals that as you increase the size of your primary aperture your spot size decreases in the far field; however, once past the focal point, determined by the range to the target, spot size once again begins to grow. A larger spot size decreases the amount of power and energy available so even these more interesting results prove that the model is functioning correctly.

The size of the secondary aperture also effects how much energy is delivered to the system. As discussed in Sect. 3.1.11 jitter induced by the secondary aperture depends on its ratio to the primary aperture. Therefore it is expected that as this ratio nears one the amount of power delivered will approach zero. This result is shown in Figure 20. Furthermore Figure 20 shows that the impact this ratio has dramatically increased above a ratio of 1/3.

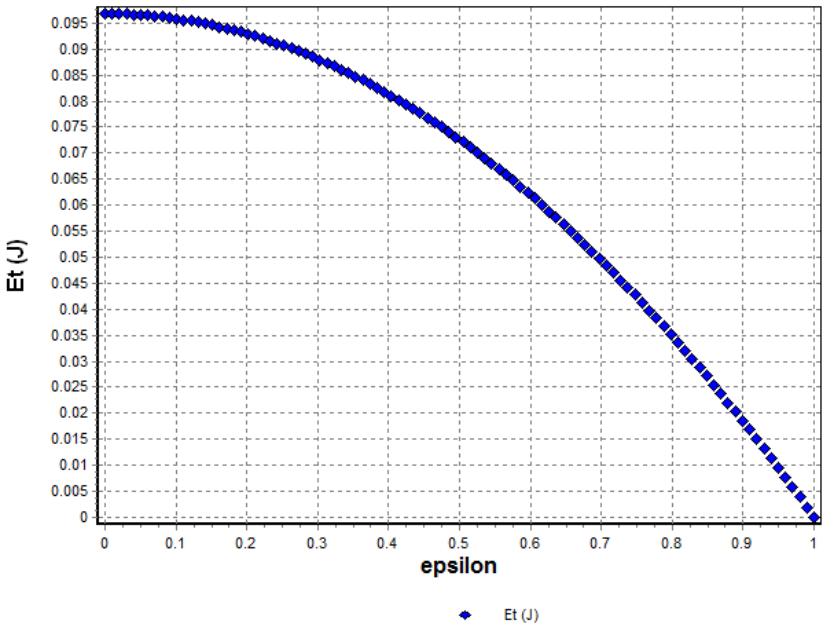

Figure 20: The Effect of the secondary to primary aperture ratio

The effectiveness of the fast steering mirror (FSM) was varied, from zero compensation of platform jitter, to total compensation of the platform jitter. As shown in Figure 21, it is only as you near total compensation that the FSM becomes effective at compensating for the platform jitter, this result is as expected from Equation (14) and Equation (15).

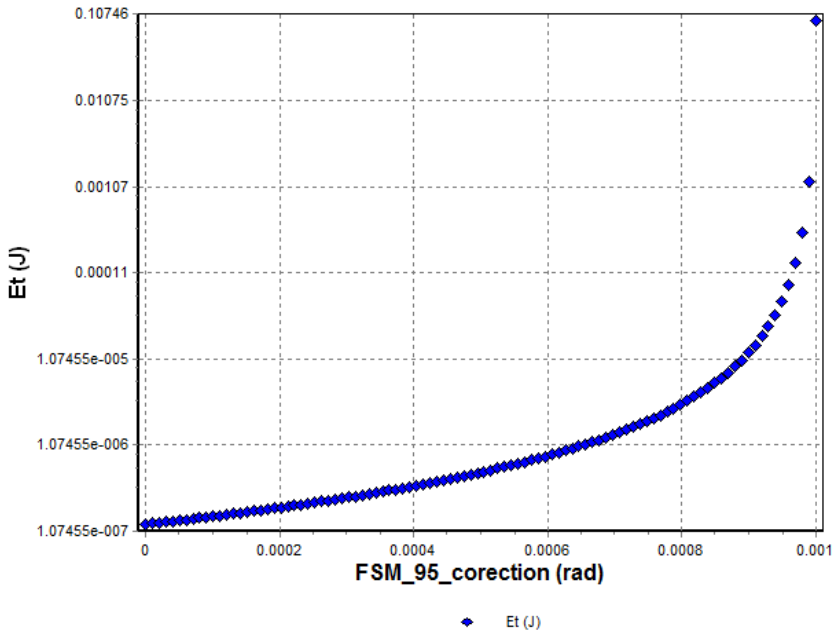

Figure 21: The effect of FSM compensation of jitter on total energy delivered

4.5 Analysis Summary

The result of the analysis indicates a working model with which aspects of a wireless power transfer system using a laser can be explored. Now that we have strong confidence that the model is functioning correctly three case studies will be performed to verify the model and show its flexibility.

4.6 Case Studies

To perform verification on the model a handful of case studies will be used in order to determine the amount of power transferred during each scenario. This will demonstrate the flexibility of the tool while providing a general idea of what is required

for a couple of current topics in the fields of space based solar power, and wireless power transfer.

Case study one will compare the results of the model to a simple hand calculation. This case study serves to verify that the model is functioning correctly and provide confidence in the results of the following case studies.

In Sect. 2.1 three different applications for wireless power transfer systems are discussed. The wireless power transfer model will be used to determine what it would take to perform two of these missions; space based solar power in Case Study 2 and power electronic propulsion in Case Study 3. These case studies will additionally serve to verify that the model does in fact model the amount of power transferred in a wireless laser power beaming experiment.

4.6.1 Hand Comparison

In order to verify that the model functions correctly, the first case study will use the model to solve a problem already solved by hand. The problem will be simplified in order to reduce the complexity of the hand calculations. Once the hand calculations are completed the model will be given the same inputs to verify that it solves for the total power delivered and the amount of time the payload can operate.

The problem assumes that a payload requiring 50 W of power is attached to an DET system using a 2500 cm^2 area GaInP/GaInAs/Ge photovoltaic array located 10 km down range of the laser system. The laser system receives 2 kW of power, has an efficiency of 25%, and emits a beam with a 1075 nm wavelength, its primary apertures

diameter is 40 cm. The laser will be engaged for 15 minutes and is considered to be well adjusted with a Strehl Ratio of 0.8. The power transfer takes place in a vacuum under daylight conditions.

To calculate by hand how long the payload can be powered given the above scenario it is first necessary to solve Equation (1) for the amount of power output by the laser beam this produces a result of 500 Watts. Solving Equation (10) for the waist of the beam w_{O2} and plug the solution into Equation (11) yields a Gaussian far-field irradiance of 435 kW/m^2 and a waist of 1.7 cm.

Applying the Gaussian irradiance to the photovoltaic cells to solve Equation (32) and Equation (22) produces a power output from the photovoltaic array of 51 W/m^2. Then solving Equation (23), Equation (24), Equation (25), and Equation (27), allows for substitution into Equation (30) to solve for the amount of time the payload can operate on the provided power. For this case the payload can operate for 19.83 minutes.

Placing the same information into the model yields a result of 19.95 minutes of operating time. There is a 0.5% difference that can be accounted for in the rounding of figures when the problem was solved by hand.

4.6.2 Space Based Solar Power.

As discussed in Sect. 2.1.1 using solar power in space to generate power for the ground has a growing following. In fact the Japanese Space Exploration Agency (JAXA) has funded a space power transfer system, intended to be operational by the year 2030, more information can be found in Sect. 2.1.1, and Sect. 2.2.2.4.

Is such an idea feasible? Could you successfully provide electric power to the ground using a solar powered laser in space? The short answer is yes, and the model demonstrates how well. For this case study it is initially assumed that an IPG Photonics YLR 1000SM, is located on board the JEM-EF. That the ISS does not prohibit look angles, the fast steering mirror can compensate for the jitter environment of the EF, and that 500 Watts of available power will be used in order to acquisition and track the receiving ground facility. It is also assumed that a 2 m^2 GaInP/GaInAs/Ge solar array is located at the Air Force Institute of Technology (AFIT), in Dayton OH to collect the power.

Now that the laser beam is passing through the atmosphere, atmospheric effects must be taken into account. Accounting for atmospheric effects can be a complicated and difficult process, but at 1060 nm the atmosphere removes less than 10% of the power in the beam (Hornyak, 2008:1). To account for this we will add a term for atmospheric Strehl to Equation (18) as shown in Equation (33):

$$I_{peak} = I_O * S_P * S_{obs} * S_{FSM} * S_{atmo} \tag{33}$$

Setting S_{atmo} to 0.9 gives a worst case scenario for atmospheric losses at this wavelength and allows us to determine how long a 100 Watt light bulb could be lit using an orbiting laser.

Inputting these values into the model and using STK to determine maximum pass time and mean range shows that for a single pass of 590 seconds the laser power beaming system is capable of lighting a 100 Watt light bulb at the AFIT ground station for about a minute.

The planned JAXA wireless power transfer system is much larger placed at an altitude of 36,000 km (Gingichashvili, 2007) it is Japan's hope that this system could power a city by delivering a giga-watt of power, the equivalent to the output of a large nuclear power plant (Hornyak, 2008:1), from a ground station powered by a satellite. Assuming a ground receiver area of 2 km^2 (Hornyak, 2008:1), the model shows that with a primary aperture of one meter, a well correct Strehl ratio, and a laser power output of 11 GW, this system could deliver a giga-watt of power to a ground site for use. As discussed in Sect. 2.1.1 JAXA still has some challenges to face before their system can become a reality.

4.6.3 Powering a BHT-200

In order to power a BHT-200 such as the one on board FalconSAT 5 either enough power must be delivered in a single transfer of power to perform the maneuver, or enough power must be transferred and stored in a series of passes to perform the maneuver.

For this case study it is assumed that an IPG Photonics YLR 1000SM, with a 40 cm primary aperture, is located on board the JEM-EF. That the ISS does prohibit look angle, the fast steering mirror can compensate for the jitter environment of the JEM-EF, and that 500 Watts of available power will be used to acquire and track the satellite. The satellite will be assumed to be identical to FalconSAT 5 including FalconSAT 5's known orbital parameters: inclination of 72^o, altitude of 650 km, and the other orbital parameters where set to zero for the purpose of establishing range and contact time over a three

month period. Power collection methods where varied in order to maximize power transferred.

Table 3 shows the effect of selecting different solar cells for use in powering a BHT-200. Table 3 clearly shows that FalconSAT 5 itself will not be able to accept power from the YLR 1000SM laser as its quantum efficiency above 980 nm is zero (Solar Energy Technologies Program (U.S.), 2007:20). Therefore the target satellite will need to replace its photovoltaic with one of the others in the chart.

Table 3: Solar Cell Impact

Case Study 3	GaAs	VMJ	GaInP/GaAs/InGaAs	Crystalline Silicon	GaInP/GaInAs/Ge
λ (nm)	1060	1060	1075	1060	1075
Quantum Efficiency (q)	0	0.55	0.86	0.06	0.9
Power Conversion Efficiency η	0.218	0.5	0.412	0.428	0.411
Total maneuver time (Tt) (s)	0	0.046	0.059	0.004	0.062

4.6.4 Powering a BHT-200 on board an optimized satellite

Case Study three is far from optimal for a space power beaming scenario therefore Case Study four will optimize Case Study three using the findings of this thesis to maximize the amount of power transferred.

For this case study it is assumed that an IPG Photonics YLR 1000SM, with a 40 cm primary aperture, is located on board the JEM-EF. That the ISS does prohibit look angle, the fast steering mirror can compensate for the jitter environment of the JEM-EF, and that 500 Watts of available power will be used to acquire and track the satellite. That

the satellite is not in eclipse at the time of the power transfer and that the satellite uses a battery to store the power until the BHT-200 is fired.

The numbers in Table 3 assume a satellite similar to FalconSAT 5 is used: that a Peak Power Transfer (PPT) model is used, a NiCd battery is used, and that a BHT-200 is the payload being powered. For the AFIT mission it is recommended that a Direct Energy Transfer (DET) power model be used on board the satellite as Figure 18 shows a 6% increase in the amount of time a BHT-200 can fire if a DET model is used instead of the PPT model. Furthermore a triple junction GaInP/GaInAs/Ge photovoltaic should be used to gather the light as Table 3 indicates it is the best suited for this type of mission.

The numbers in Table 3 also assumes a total contact time of 39 seconds after a full three months of on orbit time, using the optimized orbit developed in parallel to this work and presented in *Mission Analysis and Design for Space Based Inter-satellite Laser Power Beaming* gives the new satellite 117,251 seconds or approximately 1 day, 8 hours, and 34 minutes, of contact time over a three month period (Keller, 2010:54).

The result of these changes to Case Study 3 allows the thruster to fire for 4,226 seconds either continuously, at the end of the three months, or broken up over the three months as the mission requires.

Furthermore assuming there is room on the JEM-EF platform increasing the size of the primary aperture of the laser to a 100 cm, would deliver nearly three times as much power allowing the thruster to fire continuously for 12,770 seconds at the end of three months.

4.6.5 Case Study Summary

The above case studies serve to verify the model and provide a high level of confidence in the models output. The model can also be used in order to make recommendations about selections required when designing a wireless power transfer system.

4.7 Summary

The validated and verified model places mathematic rigor behind more than a decade's worth of academic exercises. The model can be used to show the feasibility of laser power beaming systems, from major endeavors such as the JAXA SSP system to smaller missions of powering satellite payload the model not only shows the amount of power transferred but can be used to make system level design choices.

For transferring power from the ISS to a passing small satellite the model allowed us to determine what devices should be used to receive the power, a power model for the satellite, and ideal values for aspects of the laser control system. These finding are discussed further in Chapter V.

V. Conclusions and Recommendations

The power transfer model accurately shows the amount of power that will be transferred by a laser system with a photovoltaic collector. Specific inputs are required in order to account for the type of laser, collector, and potential environmental losses such as the atmosphere.

5.1 Conclusions

These required inputs allow us to further use the model to determine what components make for the most efficient system for a specific goal. For the wireless power transfer system proposed for the ISS, certain parameters are fixed making it possible to use the model in order to make recommendations to maximize the amount of power transferred in the system.

These results show decisively that it is possible to power a satellite payload using the 3 kW power supplied by the ISS and a laser to beam the power to the satellite. The proposed experiment provides a concept demonstration for wirelessly powering electronic propulsion satellites while on orbit; the math shows conclusively that it can be done. A proof of concept will open the door for future utility lasers in the field of both Earth orbiting platforms as well as future space exploration mission on the moon and elsewhere.

5.2 Mission Design

5.2.1 Laser Recommendation

As discussed in length in Sect. 2.2.2.4 the best laser on the market today for this experiment is the IPG Photonics YLR 1000SM. This laser can be customized to output any wavelength from 1060 nm to 1080 nm, has near diffraction limited performance, and can output up to 2 kW of power (IPG Photonics Corporation, 2009b:3). This laser only weighs 150 kg (IPG Photonics Corporation, 2009b:3) and is small enough to allow for the laser control system and focusing optics.

5.2.2 Satellite Recommendations

As discussed in Sect. 3.4 three aspects of the satellite influence how much power is delivered to the BHT-200 used to demonstrate the effectiveness of the power transferred. These three items are the solar array, the onboard batteries, and the power transfer model.

As discussed in Sect. 2.4 two aspects of photovoltaic power collection have an impact on how efficiently the array gathers power. Quantum efficiency and power conversion efficiencies for each photovoltaic researched are provided in Table1. The model indicates that a triple junction solar cell with a Germanium coating designed to collect longer wavelength emissions is the most effective cell for powering BHT-200 on board a satellite as shown in Table 3. It is recommended that a similar triple junction solar cell be used for the wireless power transfer experiment in order to maximize power transfer.

The Nickel Cadmium battery on board FalconSAT 5 has 90% charge/discharge efficiency, and is already space qualified (see Appendix B for more information on batteries). It is recommended that an identical battery or set of batteries be used on board the target satellite.

As discussed in Sect. 3.4.2 a direct energy transfer (DET) power model is 5% more efficient than the Peak Power Tracking (PPT) model currently used by FalconSAT 5. To achieve the maximum power transfer it is recommended that the target satellite should use a DET model.

The payload should be capable of operating long enough for independent verification of mission success. For the BHT-200 this means raising the altitude of apogee by at least 20 meters, twice what is required in order to distinguish between a maneuver and an error in tracking the satellite (Oswieler 2006:46). To make this orbital maneuver the minimum fire time for the thruster is 54 seconds, leading to a 20 meter increase in altitude.[5] Anything less and independent verification will not be possible. To fire the thruster for 54 seconds will require no more than 2000 seconds of contact time if the previous recommendations of this work have all been implemented in the system design.

[5] For more information on how to perform these calculations see *Space Mission Analysis and Design 3rd Edition* Chapters 6 and 17

5.3 Recommendations for Future Research

The model presented here gives a reasonable understanding for the amount of power transferred by a power beaming system in space. For the sake of the research, all values used for photovoltaic cells assumed standard test conditions (STC) as outlined in section 2.3 Photovoltaic Power Collection. The lasers where also assumed to function as advertised by their respective vendors.

It is recommended that the components discussed in Sect. 5.2 be acquired and tested to determine realistic values for efficiency in an environment similar to what is expected by orbiting systems, vacuum, hot cold cycles, and the effects of launch on the system. This additional testing will determine even better values for the efficiencies for each component which can then be put into the model for an even more accurate understanding of the amount of power transferred.

It is further recommended that research be conducted on the acquisition and tracking strategy for the mission in order to determine how long contacts between the ISS and the target satellite will be and ensure that the laser system will be able to locate the target satellite.

Finally as shown in Sect. 4.4, the control system of the laser is where the biggest benefits of optimization can be realized. For this reason it is recommended that a control system be developed to maximize the amount of power transferred.

Appendix A: Satellite Acquisition Concerns.

In order to power the receiving satellite from the international space station a handful of conditions must be met. First the satellite must be within the effective range of the laser as discussed in Sect. 3.2.3. Secondly the laser must have an unobstructed view of the satellite as covered by *Mission Analysis and Design for Space Based Inter-satellite Laser Power Beaming*. Finally the laser must be able to locate the satellite.

Locating the Satellite

In order to locate the satellite mission planners can use the two line element (TLE) set from North American Aerospace Defense Command. The six orbital elements of any satellite are provided by the TLE for that satellite, therefore a two line element set can be used to predict the trajectory of the satellite by using the Simplified General Perturbation Number 4 (SGP4) analytical orbital model as in *Mission Analysis and Design for Space Based Inter-satellite Laser Power Beaming* This allows mission planners to know the satellites position and velocity vectors at a specific time in order to determine when it is within range of the laser on board the international space station.

Unfortunately, the accuracy of the TLE data is poor (Osweiler, 2006:2), in order to make up for this

> numerically derived state vectors—six independent elements which provide the position and velocity vectors in three dimension space—are often used to fine tune the selection the calculations after an initial selection with SGP4. Due to the mathematical formulation, the numerically derived state vectors have a covariance matrix associated with them,

> indicating the relative uncertainty in the solution (Osweiler, 2006:2).

A covariance matrix is a mathematical matrix used to describe the covariance between elements of a random vector. In this case it can be used to determine the probability that a satellite will be in a specific region of space (Osweiler, 2006:15). This was done by Captain Victor P. Osweiler in 2006 for his thesis Covariance Estimation and Autocorrelation of NORAD Two-Line Element Sets.

Unfortunately his method cannot be repeated in order to find the covariance matrix specific to this problem as the mission satellite has not been launched, and the tracking data needed to create the covariance method is unavailable. His data is still useful as he looked at a handful of low earth orbits similar to the one the target satellite is intended to use.

In LEO satellites atmospheric drag is the biggest contributor to increase in velocity residuals, which is the largest contributor to position error (Osweiler, 2006:52). This change in velocity induced error will only get worse through the Solar Max period, around 2012, as atmospheric drag on the satellite increases (Tascione, 1994:137) According to Osweiler "covariance for the LEO satellites exposed to drag are much larger than, [and] have little to no consistency (Osweiler, 2006:59)." If it is assumed that the target satellite behaves better than the worst case scenario that Osweiler found the laser will have a region of space to search no greater than 1150 km^2 (Osweiler, 2006:58).

Time to Acquire

Modern laser devices tend to acquire targets first by visual means, in the case of the target satellite a visual optic would stare at a known position that the satellite must pass through before the satellite is scheduled to arrive until it spots the satellite. Then the tracking laser will be engaged, and will check the surface of the satellite for the corner cube reflector. The corner cube reflector serves two purposes, first it allows the control system to positively identify the satellite as the power receiver, and second the corner cube reflector is an aim point for the high power laser. Once the corner cube reflector has been located and the system is tracking the laser. As mentioned in Sect. 5.3 more research would be required to determine how long this process will take.

Appendix B: Battery Charge Time.

During the development of the model presented here the question arose of how long must the laser have contact with the satellite in order to charge the on board Nickel Cadmium batteries?

Naturally the answer to this question is it depends. Any amount of contact time will charge the batteries with 90% (Space Systems Research Center, 2009) of the power supplied over the duration of the charge. Therefore longer charges are more efficient than shorter charges.

For example in the model power is provided by the solar cells in watts. For the baseline experiment the satellite receives 6 watts, at an average range of 566 km, and an average contact time of 4024 seconds. To get the supplied current we simply divide the number of watts by the bus voltage, 28 Volts, this gives us 214.3 mA.

This allows us to determine a charge rate for the batteries. The charge rate is the percentage of the batteries capacity delivered as current to the battery in Amp/Hr (Linden & Reddy, 2002: Chapter 1). In the baseline example, provided above, we are receiving 0.2 Amp/hr or 0.4% of the batteries capacity for the duration of the charge. This amounts to a total charge of 191 mA for this contact.

Battery Discharge

Unused batteries do discharge some of their charge over time. This can be overcome by trickle charging the batteries; however, that is not an option for a wireless

power transfer system because the power source is not continuously present for the duration that the batteries are not in use.

To ensure that there is charge buildup in the batteries compare the amount of charge over a designated time to the rate of discharge for the batteries. The Nickel Cadmium Batteries used discharge 10% of their charge capacity each month they are stored (Linden & Reddy, 2002: Chapter 26), not used and not charged, at 20^{o} Celsius. This equates to 1.2% over the average time between contacts. If we assume that the temperature is 20^{o} Celsius or less, and that the batteries discharge only in the span of time between usable contacts, then the amount of charge required during each contact to overcome the discharge effect can be determined.

For the example above each contact duration must be at least 23 seconds to overcome the discharge amount, and anything greater will positively charge the batteries on board the satellite.

Appendix C: The Effects of Sunlight on the Satellite.

As discussed in Sect. 3.2.2 the electronic power subsystem is 5% more efficient during daylight than during eclipse. For this reason it is desirable to transfer power during daylight; however, we should also be aware of the impact of sunlight on the photovoltaic cell.

Impact of sunlight on the photovoltaic cell

The irradiance of the sun on an earth orbiting satellite is 1367 W/m^2; the irradiance provided by the laser varies with range but on average is 172.6 W/m^2.

Assuming the photovoltaic is GaInP/GaInAs/Ge as recommended in Sect. 5.1.3. When only the sun is present on the solar array it will generate 60 watts, assuming a 45^o angle of incidence, and duration equal to total contact time with the laser, which will either be consumed by the satellite or used to charge its battery as dictated by the electronic power subsystem (EPS).

When only the laser is present, aka the power transfer is occurring during eclipse it will generate 5 watts, which will either be used to fire the Hall Effect Thruster, or charge the battery as determined by the EPS.

When both the sun and the laser are present, i.e. the power transfer is occurring during daylight then the two irradiances add together to generate 66 watts, 60 watts from the sun and 6 watts from the laser combined with the more efficient EPS under daylight conditions.

Appendix D: MATHCAD Code.

Given

$\eta laser := 25\%$ Input: The efficiency of the laser: according to IPG Photonics is 25%

$P := 2.5kW$ Input: Wall plug power available to the laser through the JEM EF

The beam quality for the IPG Photonics laser is 1.1 which is near diffraction limited.

$Range := 566.8927km$ Input: mean range to target in km

$\lambda := 1075nm$ Input: the wavelength of the laser can range from 1060 nm to 1080 nm according to IPG Photonics

$D := 40cm$ Input: the diameter of the primary aperture

$\tau := 4024.391s$ Input: contact or dwell time of the laser on the surface of the satellite (mean contact time from STK)

$q := 90\%$ Input: Quantum efficiency of the solar cell at the given wavelength

$\eta cell := 41.1\%$ Input: the power conversion efficiency of the laser provided by table 1.

$Id := 0.77$ Input: The nominal inherent degradation of the solar cell provided by table 1.

$\theta := 45deg$ Input: the angle of incidence at which the laser strike the solar array

$Satellite\_Life := 1$ Input: the planned lifetime of the satellite

$Annual\_Degradation := 2.75\%$ Input: the degradation per year provided in Modeling a Photovoltaic Collector.

$Asa := (20.25 \times 19.2)in^2$ Input: the Area of the solar array

$To := 2190K$ Input: the operating temperature of the laser

$Ata := 0m^2$ Input: the area of the thermal array

$PPT := 0$ $Tr := 117251.067sec$ Input: When PPT is set to one a Peak Power tracking model is being used, otherwise a Direct Energy Transfer model is being used.

$E := 0$ $Ppayload := 200W$ Input: When E is set to 1 the vehicle is in eclipse otherwise it is in sunlight.
Input: *Tr* is the amount of time the vehicle is receiving power, and P is the amount of power the BHT-200 requires.

$DoD := 20\%$ Input: The Depth of Discharge for a low earth orbiting satellite.

$Vb := 28V$ Input: The bus voltage of the target satellite, provided by the USAFA

$\eta battery := 90\%$ Input: The efficiency of the batteries, provided by the USAFA

Basic Laser Performance from Laser Performance Modeling:

$Pactual := P \cdot \eta laser$ Output: The power output of the laser

$Pactual = 625\,W$

$Wieght := \frac{Pactual}{3\frac{W}{kg}}$ Output: calculation gives best current technology achievable

$Wieght = 208.333\,kg$

Diffraction Limited Performance from Diffraction Limited Performance:

$Radiance := \frac{Pactual}{\lambda^2}$ Output: Radiance is a measure of intensity

$Radiance = 5.408 \times 10^{14} \cdot \frac{W}{sr \cdot m^2}$

$B := \frac{\pi}{4} \cdot \frac{Pactual}{\left(\frac{\lambda}{D}\right)^2}$ Output: Brightness is a range independent measure of merit

$B = 6.796 \times 10^{13} \cdot \frac{W}{sr}$

$Io := \frac{B}{Range^2}$ Output: the diffraction limited maximum amount of irradiance

$Io = 211.481 \cdot \frac{W}{m^2}$

$$Aeff := \frac{Pactual}{Io} = 2.955\,m^2$$

Output: Beam area is the diffraction limited 2d cross sectional area the laser encompasses in the far field

$$Aeff = 2.955\,m^2$$

$$rd := \sqrt{\frac{Aeff}{\pi}}$$

Output: The diffraction limited waist or the beam radius is the far field measurement used to relay the size of the laser at the target.

$$rd = 0.97\,m$$

Spot Size determination from **Determining Spot Size**:

$$wo2 := \sqrt{\frac{1}{\frac{4}{D^2} + \left(\pi \cdot \frac{D}{2 \cdot Range \cdot \lambda}\right)^2}}$$

Target Waist assuming focal length=range, 2wo1=D and zr<<f (See slide 90 of laser physics)

Irradiance from **Gaussian Irradiance:**

$$I := \frac{\pi \cdot Pactual \cdot D^2}{4 \cdot Range^2 \cdot \lambda^2}$$

The Gaussian Irradiance in the far field

Sources of Beam degradation from **Strehl, Strehl due to Platform Jitter**, **Strehl due to Obscuration**, **Compensating for Strehl with a Fast Steering Mirror**:

$$\theta\_jit := 10^{-3}rad \quad -0.001rad$$

The jitter of the EF attached to the JEM corrected by the FSM

$$\sigma\_jit := \frac{\theta\_jit}{\frac{\lambda}{D}}$$

The jitter expressed as a Gaussian shape

$$Sjit := \frac{1}{1 + \frac{\pi^2}{2} \cdot (\sigma\_jit)^2}$$

Strehl caused by platform jitter

$$\varepsilon := \frac{10cm}{40cm}$$

The Obscuration caused by secondary aperture is equal to the ration of the diameter of the secondary aperture to the diameter of the primary aperture

$Sobs := 1 - \varepsilon^2$ Strehl caused by obscuration

$\theta\_fsm := 0.000001rad$ Quiescent Jitter caused by the fast steering mirror

$\sigma\_fsm := \frac{\theta\_fsm}{\frac{\lambda}{D}}$ The quiescent jitter expressed as a Gaussian Shape

$Sfsm := e^{-\sigma\_fsm^2}$ Strehl induced by the fast steering mirror

$Satmo := 1$ Atmospheric losses at 1060 nm = 0.9

Peak irradiance or power in the bucket

$Ipeak := I \cdot Sjit \cdot Sobs \cdot Sfsm \cdot Satmo$

Output: *Ipeak* is the irradiance in the far field according to the Gaussian model. It is the irradiance on the solar panel

$Ipeak = 172.629 \cdot \frac{W}{m^2}$

Fluence Check:

An attempt to make sure we don't harm the satellite.

$Fluence := Ipeak \cdot \tau$

The Fluence Delivered; lethal fluence for a satellite is considered to be 50-500 J/cm^2.

$Fluence = 69.473 \cdot \frac{J}{cm^2}$

Photovoltaic Power Collection from Modeling a Photovoltaic Collector:

Quantum Losses from:

$I := Ipeak \cdot q$

$I = 155.366 \cdot \frac{W}{m^2}$ Irradiance provided by laser after quantum losses

$Po := \eta cell \cdot I$ The power output of the photovoltaic cells

$Pbol := Po \cdot Id \cdot \cos(\theta)$ Power required at the beginning of life from the solar array

$Ld := (1 - Annual\_Degradation)^{Satellite\_Life}$ Lifetime degradation of the solar cells

$Peol := Pbol \cdot Ld$ Power required at the end of life from the solar array

$Psa := Peol \cdot Asa$ The power we get from the solar array

Thermal Power Collection

$Ts := 2300K$ The stagnation temperature of modern thermal systems

$Ta := 4K$ The ambient temperatures of the thermal environment, roughly 4 K for outer space, see **Modeling a Thermal Collector**

$\eta := \frac{Ts^4 - To^4}{Ts^4 - Ta^4}$ The efficiency of the thermal collector is given by η

$Pta := \eta \cdot Ipeak \cdot Ata$ The power provided by the thermal array

Satellite System Losses from Modeling Losses Inherent in EPS:

$Tt :=$ if PPT
  $Xe \leftarrow 60\%$
  $Xd \leftarrow 80\%$
otherwise
  $Xe \leftarrow 65\%$
  $Xd \leftarrow 85\%$
$Tt \leftarrow \frac{[(Psa + Pta) \cdot Tr \cdot Xe]}{Ppayload}$ if E
$Tt \leftarrow \frac{[(Psa + Pta) \cdot Tr \cdot Xd]}{Ppayload}$ otherwise

Output: *Tt* is the amount of time the BHT thruster can be powered on with the power available from the laser.

$Pt :=$ if PPT
  $Xe \leftarrow 60\%$
  $Xd \leftarrow 80\%$
otherwise
  $Xe \leftarrow 65\%$
  $Xd \leftarrow 85\%$
$Pt \leftarrow (Psa + Pta) \cdot Xe$ if E
$Pt \leftarrow (Psa + Pta) \cdot Xd$ otherwise

$Tt = 4.226 \times 10^3 s$

$Pt = 7.209 \cdot W$

$Et := Pt \cdot Tr$

$Et = 8.453 \times 10^{5}\,J$

Battery Capacity from Modeling Power Storage:

$$Cr := \frac{Ppayload \cdot Tt}{DoD \cdot \eta battery}$$

Output: the battery capacity required to store the power provided by the laser

$Cr = 1.304 \times 10^{3} \cdot W \cdot hr$

$$Crv := \frac{Cr}{Vb}$$

Output: To get the answer in Amp hrs simply divides *Crv* by *Vb*

$Crv = 46.586 \cdot A \cdot hr$

Bibliography

Barnett, A., Honsberg, C., Kirkpatrick, D., Kurtz, S., Moore, D., Salzman, D., et al.. "50% Efficient Solar Cell Architectures and Designs." *IEEE* , 5:2560-2564 2006.

Bartell, Richard Dayton, OH, Personal correspondence. October-December 2009.

Black, Jonathan T. Course Notes, ASYS 631 Spacecraft Systems Engineering. School of Engineering and Management. Air Force Institute of Technology, Wright Patterson AFB, OH. Spring Quarter 2009.

Cheney, M. *Tesla Man Out of Time.* New York: Dorset Press 1989.

Cobb, Richard G. Professor, Air Force Institute of Technology, Wright Patterson AFB OH. Personal correspondence. 5 March 2010.

Cusumano, Salvatore J. Course Notes, OENG 520 Laser Weapon System Short Course. School of Engineering and Management. Air Force Institute of Technology Wright Patterson AFB, OH. Winter Quarter 2009

Cusumano, Salvatore J. Director Center for Directed Energy, Air Force Institute of Technology, Wright Patterson AFB OH., Personal correspondence. October-December 2009.

Fork, R. L.. "Laser Power Beaming Demo Prelimanary Design Review" Report to NASA Personnel, Huntsville AL, 6 November 2008.

Frahrenbruch, A. L. *Fundamentals of Solar Cells.* New York: Academic Press, 1983.

Geisz, J. F., Kurtz, S. M., Wanlass, M. W., Ward, J. S., Duda, A., Friedman, D. J., et al. "High-efficiency GaInP/GaAs/InGaAs triple-junction solar cells grown inverted with a metomorphic bottom junction." *Applied Physics Letters*, 91:023502-1-3 2007

Gingichashvili, S. "Generating Power in Space." article n. pag. http://thefutureofthings.com/news/1013/generating-power-in-space.html. 16 December 2009

Goldstein, J. C. "High Power Free-Electron Laser Concepts and Problems." *Proceedings of the SPIE Laser Power Beaming II* 32-44. San Jose, CA: SPIE-The International Society forOptical Engineering, 1995.

Guter, W., Schone, J., Phillips, S. P., Steiner, M., Siefer, G., Wekkeli, A., et al. "Current-matched triple-junction solar cell reaching 41.1% conversion efficiency under concentrated sunlight." *Applied Physics Letters,* 94:223504-1-3. 2009.

Herbert Friedman, G. A. "Scaling of Solid State Lasers for Satellite Power Beaming." *Proceedings of the SPIE Laser Power Beaming* 49-57. Los Angeles, CA: SPIE--The International Society for Optical Engineering, 1994.

Hornyak, T. (2008, July). *Farming Solar Energy in Space. article. 2.* http://www.scientificamerican.com/article.cfm?id=farming-solar-energy-in-space 18 December 2009

IPG Photonics Corporation. High Power Fiber Lasers for Industrial Applications. Oxford, MA: IPG Photonics Corporation. (2009).

IPG Photonics Corporation. YLR-SM Series. Oxford, MA: IPG Photonics Corporation. (2009).

Keller, Nicholas. *Mission Analysis and Design for Space Based Inter-satellite Laser Power Beaming.* MS thesis, AFIT/GA/ENY/10-M05 School of Engeering and Management Air Force Institute of Technology (AU), Wright Patterson AFB OH, March 2010.

Landis, G. A. "Applications for Space Power by Laser Transmission." *Proceedings of the SPIE Laser Power Beaming* 252-256. Los Angeles, CA : SPIE-The International Society for Optica Engineering 1994.

Linden, D., & Reddy, T. B. *Handbook of Batteries 3rd Edition.* New York: McGraw-Hill, 2002.

Luque. *Solar Cells and Optics for Photovoltaic Concentration.* Bristol and Philadelphia: Adam Hilger, 1989

Mankins, John C.. Energy From Orbit. *adAstra: The Magazine of the National Space Society*, 5:20-24,59 (Volume 20 Issue 1, 2008)

Meschede, D. *Optics, Light and Lasers 2nd edition.* Morlenbach: Strauss GmbH, 2007

Microwave Antenna Theory and Design. London: P. Peregrinus on behalf of the institution of Electrical Engineers, 1984.

Monroe, D. K. "Laser Power Beaming to Extend Lives of GSO NiCd Satellites." *Proceedings of the SPIE Laser Power Beaming* 256-263. Los Angeles, CA: SPIE-The International Society for Optical Engineering 1994.

Monroe, D. K. "Space Debris Removal Using a High Power Ground Based Laser." *Proceedings of the SPIE Laser Power Beaming* 276-283. Los Angeles, CA: SPIE The International Society for Optical Engineering 1994.

Nufern. *Nufern Kilowatt Level Laser Amplifier Spec Sheet.* Spec Sheet 2, http://www.nufern.com/specsheets/NukW_flyer.pdf. 28 October 2009

Nufern. *Specialty Fibers and Fiber Lasers.* Home Page, n. pag. http://www.nufern.com/ 28 October 2009

Osweiler, V. P. (2006). *Covariance Estimation and Autocorrelation of NORAD Two Line Element Sets.* MS thesis, AFIT/GSS/ENY/06-M09 School of Engeering and Management Air Force Institute of Technology (AU), Wright Patterson AFB OH, March 2010.

Perram, Glen. Course Notes, OENG 520 Laser Weapon System Short Course. School of Engineering and Management. Air Force Institute of Technology Wright Patterson AFB, OH. Winter Quarter 2009

Reiman, D. "Scanning the Past: A History of Electrical Engineering from the Past." n. pag. *IEEE (Vol. 81, No. 6,* 1993).

Sandia Corporation. "*The Photovoltaic Effect*." article n. pag. http://photovoltaics.sandia.gov/docs/PVFEffIntroduction.htm. 15 December 2009

Sater, Bernard A. Sater, Neil D. "*High Voltage Silicon VMJ cells for up to 1000 Suns Intensities."* 4 Srongsville, OH: PhotoVolt, Inc. 2008.

Sater, Bernard A. PhotoVolt, Inc, Strongville OH, Personal correspondence. 14 May 2009.

Solar Energy Technologies Program (U.S.) "*DOE Solar Energy Technologies Program Fiscal Year 2007 Annual Report."* Washington, D.C.: U.S. Dept. of Energy, Energy Efficiency and Renewable Energy. September 2007.

Space Systems Research Center. "FalconSAT 5 Critical Design Review." Report to Air Force Research Laboratory Personnel, U.S. Air Force Academy, Colorado Springs, CO. December 2007.

Space Technology Library. *Space Mission Analysis and Design.* New York, NY: Microcosm Press 2008.

SPI Lasers. (2009). *DatasheetsSM-S00088.* Data Sheets 2, http://www.spilasers.com/ 27 October 2009

Sprangle, P., Ting, A., Joseph, P., Fischer, R., & Bahman, H. (2008, July 21). "BEAM COMBINING: High-power fiber-laser beams are combined incoherently." Laser Focus World article, n. pag. http://www.laserfocusworld.com/articles/331428 26 October 2009

Tascione, T. F. *Introduction to the Space Enviroment 2nd Edition.* Malabar, Florida: Krieger Publishing Company 1994.

Totty, M. (2009, October 20). "Five Technologies that Could Change Everything" Yahoo Finance article, n. pag. http://finance.yahoo.com/career-work/article/107987/five-technologies-that-could-change-everything 26 October 2009

University of Delaware Office of Public Relations. "UD-led team sets solar cell record, joins DuPont on $100 million project." PR release n. pag. http://www.udel.edu/PR/UDaily/2008/jul/solar072307.html 10 July 2009

Victor Khitrov, B. S. "242W single -mode CW fiber laser operating at 1030nm." *Optical Society of America* , 3:n. pag. (2005).

Wie, Bong. *Space Vehicle Dynamics and Control 2nd Edition.* Reston, VA: American Institute of Aeronautics and Astronautics, Inc. 2008.

Wiesel, W. E. Professor, Air Force Institute of Technology, Wright Patterson AFB OH. Personal correspondence. 7 July 2009.

REPORT DOCUMENTATION PAGE

Form Approved
OMB No. 074-0188

1. REPORT DATE *(DD-MM-YYYY)*	2. REPORT TYPE	3. DATES COVERED *(From – To)*
25-03-2010	Master's Thesis	March 2009 – March 2010

TITLE AND SUBTITLE

Minimizing Losses in a Space Laser Power Beaming System

5a. CONTRACT NUMBER

5b. GRANT NUMBER

5c. PROGRAM ELEMENT NUMBER

6. AUTHOR(S)

Bellows, Charlie T., Captain, USAF

5d. PROJECT NUMBER

5e. TASK NUMBER

5f. WORK UNIT NUMBER

7. PERFORMING ORGANIZATION NAMES(S) AND ADDRESS(S)
Air Force Institute of Technology
Graduate School of Engineering and Management (AFIT/ENY)
2950 Hobson Way, Building 640
WPAFB OH 45433-8865

8. PERFORMING ORGANIZATION REPORT NUMBER

AFIT/GSS/ENY/10-M02

9. SPONSORING/MONITORING AGENCY NAME(S) AND ADDRESS(ES)
Dr. Raymond F. Beach NASA Glenn Research Center
21000 Brookpark Road
Cleveland, OH 44135
(216) 433-5320, raymond.f.beach@nasa.gov

10. SPONSOR/MONITOR'S ACRONYM(S)

11. SPONSOR/MONITOR'S REPORT NUMBER(S)

12. DISTRIBUTION/AVAILABILITY STATEMENT
APPROVED FOR PUBLIC RELEASE; DISTRIBUTION UNLIMITED.

13. SUPPLEMENTARY NOTES

14. ABSTRACT

A mathematical model is developed to track the amount of power delivered in a wireless laser power beaming system. In a wireless system the power proceeds through several different stages before being delivered to a payload for use. Each of these stages results in power losses that are thoroughly examined, allowing for the calculation of the likely amount of power delivered. Adjusting variable factors within the model allows for the optimization of the system for a specific task. The model shows that an optimized wireless power transfer system can deliver enough power to meet the space experiment objectives. For example to power a Hall-Effect Thruster a laser, photovoltaic cells, satellite power distribution model, and batteries all impact the amount of power delivered. Careful selection of all of these components will allow the laser to power the thruster and the model provides how much power is transferred. Knowledge of the power requirements for the payload further allows the model to determine how long it will be able to operate the payload with the power provided. This model will allow system engineers to answer important design questions about the selection of components to ensure that the end product delivers maximum power.

15. SUBJECT TERMS
Laser, Space, Modeling, Optimization, Wireless, Power

16. SECURITY CLASSIFICATION OF:			17. LIMITATION OF ABSTRACT	18. NUMBER OF PAGES	19a. NAME OF RESPONSIBLE PERSON
a. REPORT	b. ABSTRACT	c. THIS PAGE			Jonathan Black, Dr., USAF, ADVISOR
U	U	U	UU	115	19b. TELEPHONE NUMBER *(Include area code)* (937) 255-6565, ext 4578 (emailname@afit.edu)

Standard Form 298 (Rev. 8-98)
Prescribed by ANSI Std. Z39-18